

SPECTROSCOPIC EXAMINATION OF THE ELECTRON TRANSFER STEP FOR

E. COLI [2FE-2S] CLUSTER BIOSYNTHESIS

A Thesis

by

ELISA NICOLE FERRARA

Submitted to the Graduate and Professional School of
Texas A&M University
in partial fulfillment of the requirements for the degree of

MASTER OF SCIENCE

Chair of Committee,	David P. Barondeau
Committee Members,	Tadhg P. Begley
	Margaret Glasner
	Paul A. Lindahl
Head of Department,	Simon W. North

December 2021

Major Subject: Chemistry

Copyright 2021 Elisa Ferrara

ABSTRACT

The excursion into biological iron-sulfur cluster assembly began at the close of the 20th century, and has continued to develop in the last twenty years. Currently, it is known that [2Fe-2S] clusters are assembled through the work of a cysteine desulfurase, which liberates sulfur from cysteine that is subsequently transferred to a scaffold protein housing iron, where electrons are then transferred to complete the [2Fe-2S] cluster. This system has been researched at length and tremendous progress has been made to uncover finer details of this process. However, gaps in knowledge still remain, primarily concerning the source of electrons and the mechanism by which they are donated to complete cluster assembly. A small [2Fe-2S] redox protein, ferredoxin, has been postulated to be the biological reductant, but evidence that conclusively establishes its behavior in this role is minimal. In spite of this, it has oft been cited as the definitive reductant for this process. To address this dearth in the field, spectroscopic techniques were employed in the *E.coli* model to assess the behavior of this ferredoxin (Fdx). UV-Visible spectroscopic assays reveal that the mechanism of electron donation from Fdx touted in the field is not catalytically competent for iron-sulfur cluster assembly, as a previously unexplored lag phase in redox activity was uncovered. With further excursions incorporating circular dichroism spectroscopy, Fdx is affirmed to serve as a physiological reductant. The results obtained challenge previously proposed facets of its behavior and shed light on its activity within in vitro settings, while also exploring the possibility of a secondary reductant at play in the cellular antioxidant glutathione.

ACKNOWLEDGEMENTS

I would like to thank my advisor, Dr. David Barondeau, and my committee members Dr. Tadhg Begley, Dr. Paul Lindahl and Dr. Margaret Glasner, for their guidance, assistance, and support throughout the course of this research. I especially would like to thank Dr. Glasner for so graciously joining my committee on such short notice. I am also incredibly grateful to Dr. Begley for allowing access to his circular dichroism spectrophotometer, which was used to conduct all circular dichroism experiments discussed in this thesis. I will forever be grateful for the opportunity to work in Dr. Barondeau's laboratory, which has allowed me to grow and develop as a young scientist.

I would also like to extend thanks to the members of the Barondeau group both past and present, who have imparted great insight and have offered incredible assistance, encouragement, and friendship during my time as a graduate student. I express additional gratitude to Dr. Cheng-Wei Lin and Syuan-Ting Kuo for performing the mass spectrometry analysis discussed in this work. Additional thanks is owed to my colleagues, the department faculty, and staff of the university for making my time at Texas A&M University a pleasant experience.

I would like to thank my mother, father, and brother for all of their encouragement and love during my graduate tenure. They have always supported my scientific pursuits, and for that, I am eternally grateful. I would also like to thank my partner, who has been my steadfast supporter and greatest friend throughout this time. Lastly, I would like to

express appreciation towards my cats for their companionship, which was a source of great comfort during difficult times.

CONTRIBUTORS AND FUNDING SOURCES

Contributors

This work was supervised by a thesis committee consisting of Dr. David P. Barondeau, Dr. Tadhg P. Begley, and Dr. Paul A. Lindahl of the Department of Chemistry, along with Dr. Margaret Glasner of the Department of Biochemistry and Biophysics.

The mass spectrometry data presented and discussed in section 2.3 was provided through the work and analysis of by Dr. Cheng-Wei Lin and Syuan-Ting Kuo of the Department of Chemistry. Circular dichroism experiments were conducted using the Applied Photophysics spectrophotometer courtesy of Dr. Tadhg Begley.

All other work conducted for the thesis was completed by the student independently.

Funding Sources

This work was made possible by the NIH under Grant Number R01GM096100, the NSF under Grant Number CHE 1508269, and the Robert A. Welch Foundation under Grant Number A-1647. Its contents are solely the responsibility of the authors and do not necessarily represent the official views of the NIH, NSF or Robert A. Welch Foundation.

NOMENCLATURE

CD	Circular Dichroism
DMPO	5,5-dimethyl-1-pyrroline-N-oxide
DTT	Dithiothreitol
DT	Dithionite
Fdx	<i>E. coli</i> [2Fe-2S] ferredoxin
GSH	Reduced glutathione
GSSG	Oxidized glutathione
Grx4	<i>E. coli</i> glutaredoxin
IscS	<i>E. coli</i> cysteine desulfurase
IscU	<i>E. coli</i> iron-sulfur cluster assembly scaffold protein

TABLE OF CONTENTS

	Page
ABSTRACT	ii
ACKNOWLEDGEMENTS	iii
CONTRIBUTORS AND FUNDING SOURCES.....	v
NOMENCLATURE.....	vi
TABLE OF CONTENTS	vii
LIST OF FIGURES.....	viii
1. INTRODUCTION.....	1
2. SPECTROSCOPIC ANALYSIS OF ELECTRON TRANSFER IN <i>E. COLI</i> IRON-SULFUR CLUSTER ASSEMBLY	17
2.1. Introduction	17
2.2. Experimental Procedures.....	19
2.3. Results	25
2.4. Discussion	45
3. CONCLUSIONS.....	50
REFERENCES.....	52

LIST OF FIGURES

	Page
Figure 1.1 Different stoichiometries of various iron-sulfur clusters. Reprinted with permission from <i>Nature Chemical Biology</i> , 2(4): 171-174. Copyright 2006 Nature Publishing Group.	1
Figure 1.2 Depiction of the ISC operon in E. coli. Reprinted with permission from <i>Biochim. Biophys. Acta Mol. Cell Res.</i> 2015, 1853 (6), 1416–1428. Copyright © 2014 Published by Elsevier B.V.	3
Figure 1.3 Crystal structure of E. coli Fdx with its [2Fe-2S] cluster bound... ..	5
Figure 1.4 Structure of holo-Fdx, residues highlighted in green exhibit the greatest extent of perturbation seen in NMR when IscS is present. Adapted from <i>J. Biol. Chem.</i> 2013, 288 (34), 24777–24787.	8
Figure 1.5 Proposed HADDOCK model of a Fdx-IscS complex and electrostatic potential map of the Fdx-IscS binding region. Adapted from <i>J. Biol. Chem.</i> 2013, 288 (34), 24777–24787.	9
Figure 1.6 Proposed HADDOCK model of a hypothetical ternary complex of Fdx-IscS-IscU. Adapted from <i>J. Biol. Chem.</i> 2013, 288 (34), 24777–24787.	9
Figure 1.7 Time resolved circular dichroism spectroscopy of the formation of holo-Isu1. Elimination of Yah1 and its reductase attenuate the extent of [2Fe-2S] synthesis. Reprinted with permission from Springer Nature [Nature Communications] [<i>Nat. Commun.</i> 5:5013.] Copyright 2014 Springer Nature... ..	10
Figure 1.8 Time resolved UV-Visible spectra of reduced Fdx, IscS, and cysteine, along with reduced Fdx, IscS, IscU, cysteine, and Fe ²⁺ over the course of 30 minutes post addition of L-cysteine. Reprinted with permission from <i>J. Am. Chem. Soc.</i> 2013, 135, 8117–8120. Copyright 2013 American Chemical Society..	12
Figure 1.9 Time resolved UV-Visible spectra highlighting the change in oxidation state for FDX1 and FDX2 respectively with cysteine desulfurase and L-cysteine or cysteine desulfurase, L-cysteine, the scaffold protein, and Fe ²⁺ . Reprinted with permission from <i>Biochemistry</i> 2017, 56, 487–499. Copyright 2017 American Chemical Society.	13
Figure 1.10 Persulfidation assay conducted with NSF1 and ISCU2 in the presence of reduced FDX2. Persulfidated NFS1 and ISCU2 were identified through a	

maleimide peptide assay. SDS PAGE gels depict the presence of persulfides on NFS1 and ISCU2, as indicated by the arrows. Only the persulfide on ISCU2, not NSF1, was reduced by FDX2. Adapted from *Nat Commun* 10, 3566 (2019).....14

Figure 2.1 Time-resolved UV-Visible spectroscopy of 50 μ M reduced Fdx, 50 μ M IscS, and 250 μ M L-cysteine over 30 minutes. Each trace represents the spectra collected at every minute. The initial spectrum of reduced Fdx is indicated by the bottom red trace. The overall direction of the change in the spectra over time is indicated by the arrow, with the emergence of the “double hump” at 414 nm and 456 nm characteristic of Fdx oxidation. Contribution from IscS was removed prior to collection of spectra.....27

Figure 2.2 50 μ M reduced Fdx in the presence of 250 μ M L-cysteine and in the presence of 50 μ M IscS. Spectra presented are the overlay of individual traces over 30 minutes. In these control experiments, the absence of peaks at 414 nm and 456 nm indicates that neither L-cysteine nor IscS alone are sufficient to oxidize Fdx.27

Figure 2.3 The change in absorbance at 456 nm monitored over the course of 30 minutes as a means of tracking the oxidation of Fdx. The plot was generated from the average of 3 experiments conducted in the manner of that seen in Figure 2-1. Note the delay in Fdx oxidation, the observable lag phase was found to average roughly 5 minutes for this set of experiments.....28

Figure 2.4 Time resolved UV-Visible spectroscopy of 10 μ M reduced Fdx, 10 μ M IscS, and 50 μ M L-cysteine. Each trace represents the spectra collected at every minute. The initial spectrum of reduced Fdx is indicated by the bottom red trace. The overall change in the spectra is indicated by the arrow, with the emergence of the “double hump” at 414 nm and 456 nm characteristic of Fdx oxidation. Contribution from IscS was removed prior to collection of spectra... ..29

Figure 2.5 The change in absorbance at 456 nm monitored over the course of 30 minutes as a means of tracking the oxidation of Fdx. The plot was generated from the average of 3 experiments conducted in the manner of that seen in Figure 2-4. Note the delay in Fdx oxidation, the observable lag phase was found to average roughly 10 minutes for this set of experiments.....29

Figure 2.6 Time resolved UV-Visible Spectroscopy of 10 μ M reduced Fdx, 10 μ M IscS C328A, and 50 μ M L-cysteine along with 10 μ M reduced Fdx, 10 μ M IscS, 50 μ M L-cysteine, and 2 mM TCEP . Each trace represents the spectra collected at every minute. The lack of the characteristic double hump at 414 nm and 456 nm signifies that under these conditions, Fdx was unable to oxidize. Contributions from IscS were removed prior to collection of spectra.....	31
Figure 2.7 10 μ M oxidized Fdx in the presence of 2 mM TCEP. Spectra presented are the overlay of individual traces over 30 minutes. The persistence of the peaks at 414 nm and 456 nm indicates that TCEP is not a reductant capable of reducing Fdx.....	31
Figure 2.8 Time resolved UV-Visible spectroscopy of 10 μ M reduced Fdx, 10 μ M IscS C110A/C170A, and 50 μ M L-cysteine. Each trace represents the spectra collected at every minute. The overall change in the spectra is indicated by the arrow, with the emergence of the “double hump” at 414 nm and 456 nm characteristic of Fdx oxidation, which is unaffected by the utilization of this mutant form of IscS. Contribution from IscS was removed prior to collection of spectra.....	32
Figure 2.9 The change in absorbance at 456 nm monitored over the course of 30 minutes as a means of tracking the oxidation of Fdx. The plot was generated from the average of 3 experiments conducted in the manner of that seen in Figure 2-7. Note the lack of a considerable delay in Fdx oxidation, as it appeared to readily transpire under these conditions.....	32
Figure 2.10 UV-Visible comparison of Fdx oxidation in the presence of proteinaceous persulfide and non-proteinaceous persulfide. Assays were conducted with 10 μ M IscS and various concentrations of L-cysteine, which were preincubated together prior to separation with a spin concentrator. 10 μ M reduced Fdx was added to the two separate components and examined with UV-Visible spectroscopy. The persulfide localized on IscS readily reduced Fdx, whereas the non-proteinaceous component failed to do the same. Traces followed the change at 456 nm and were the average of at least 2 or more experimental trials.....	34
Figure 2.11 Comparison of average lag times before the advent of Fdx oxidation in UV-Visible assays conducted with 10 μ M reduced Fdx, 10 μ M IscS or IscS C110A/C170A and various concentrations of L-cysteine. A consistent trend emerges in which greater concentrations of cysteine correlate with long lag phases before Fdx oxidation transpires. There was no discernable difference observed between studies conducted with WT IscS or the double mutant. Averages were taken from experiments conducted in triplicate.....	35

Figure 2.12 Comparison of average lag times before the advent of Fdx oxidation in UV-Visible assays conducted with 10 μ M IscS, and various concentrations of L-cysteine that had been incubated 30 minutes prior to the addition of 10 μ M reduced Fdx . Lag phases were found to attenuate or disappear entirely as a result of preincubation of IscS and cysteine. Averages were taken from experiments conducted in triplicate.....	36
Figure 2.13 List of reactions at play in the assays conducted in Figures 2-1 to 2-12. 1) is the cysteine desulfurase activity of IscS that removes the thiol group from cysteine to generate alanine, creating a persulfide on the catalytic cysteine of IscS. 2) represents a potential side reaction between cysteine and IscS persulfide, in which cysteine behaves as a thiol reductant to cleave the persulfide on IscS. 3) represents the interaction between IscS and reduced Fdx, in which Fdx reduces the persulfide on IscS. When cysteine is present in excess, it is possible that reaction 2 supplants reaction 3, possibly explaining the lengthening lag phase of Fdx oxidation under these conditions.....	37
Figure 2.14 Circular dichroism spectra of holo-IscU, reduced Fdx, and oxidized Fdx. Holo-IscU formation is monitored at 330 nm, whereas oxidation of Fdx is observed through an increase in ellipticity in the region of 400-450 nm... ..	38
Figure 2.15 Time resolved circular dichroism spectroscopy of iron-sulfur cluster assembly on IscU. All reactions contained 30 μ M IscU, 2 μ M IscS, 100 μ M L-cysteine, and 250 μ M ferrous iron, with concentrations of reduced and oxidized Fdx varied. Formation of [2Fe-2S] clusters was monitored via 330 nm, and the extent of cluster formation was found to be greatest under conditions with stoichiometric quantities of reduced Fdx.... ..	39
Figure 2.16 Time resolved circular dichroism spectroscopy of iron-sulfur cluster assembly on IscU. All reactions contained 30 μ M IscU, 2 μ M IscS, 100 μ M L-cysteine, and 250 μ M ferrous iron, with variations in the concentrations of reduced Fdx, and/or 2 mM GSH. Formation of [2Fe-2S] clusters was monitored via 330 nm, and the extent of cluster formation was found to be greatest under conditions with both GSH and reduced Fdx. However, GSH alone was found to facilitate iron-sulfur cluster assembly to a greater degree than reduced Fdx alone.	41
Figure 2.17 Time resolved circular dichroism spectroscopy of [2Fe-2S] cluster assembly and transfer. Assays were conducted with 30 μ M IscU, 2 μ M IscS, 30 μ M Grx4, 100 μ M L-cysteine, 250 μ M ferrous iron, and 10 mM GSH. Spectra were collected over the course of 2 hours post reaction initiation, with each trace collected every 10 minutes. The second spectrum was collected 12 hours after the reaction initiation... ..	43

Figure 2.18 Mass spectrum obtained from denaturing conditions of IscS. Experimental conditions featured 10 μ M IscS, 10 μ M reduced Fdx, 50 μ M Cys, and 1 mM DMPO. The major peak observed is apo-IscS, or IscS with no persulfide or adduct on its catalytic cysteine. This peak, with a m/z of 3445.33, is the only peak of significant intensity. No mass shifts corresponding to the mass shift of a DMPO adduct were detected.....	44
Figure 2.19 Proposed model of Fdx mediated reduction for iron-sulfur cluster assembly on IscU.....	47
Figure 2.20 Proposed model of GSH mediated iron-sulfur cluster assembly.....	48

1. INTRODUCTION

Iron-sulfur clusters are ancient inorganic cofactors ubiquitous to all kingdoms of life. Said to be relics of the “iron-sulfur world”, these versatile prosthetic groups exist in several different stoichiometries, ranging from [2Fe-2S], [3Fe-4S], to [4Fe-4S], as viewed in Figure 1-1.¹ Plasticity in form imbues iron-sulfur clusters with a great degree of functional diversity, as the proteins in which they associate with are involved in myriad key biological processes: cellular respiration, DNA replication and repair, iron sensing, and protein regulation among others.¹⁻⁵ The continued existence of iron-sulfur clusters in organisms both simple and complex is a testament to these cofactors’ irreplaceable nature in such critical roles.

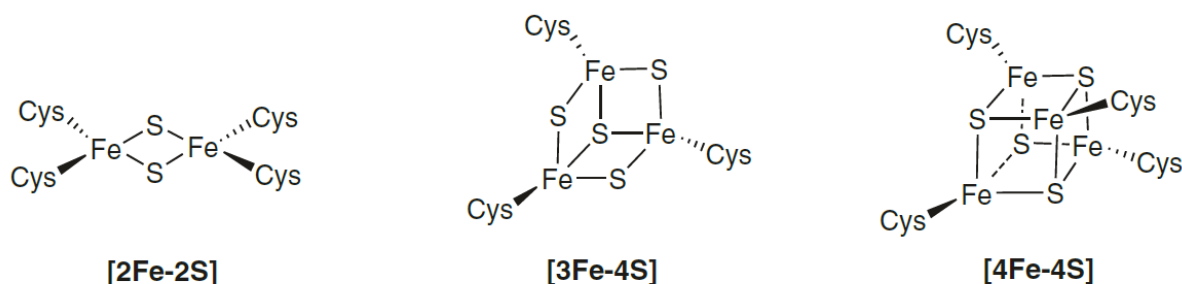


Figure 1-1. Different stoichiometries of various iron-sulfur clusters. Reprinted with permission from *Nature Chemical Biology*, 2(4): 171-174. Copyright 2006 Nature Publishing Group.

While the role of multitudinous iron-sulfur cluster proteins have been elucidated over the past 50 years, there remains a gap in knowledge concerning the biological processes behind their physiological assembly. Insight into the biological synthesis of iron-sulfur clusters began at the close of the 20th century, heralded by the discovery of the ISC operon of *A. vinelandii* in 1998 by the Dennis Dean laboratory.⁶ Perturbations of the proteins associated with this operon and other gene clusters subsequently manifested in the attenuation of the quantity of iron-sulfur cluster proteins, providing evidence that iron-sulfur clusters are synthesized through an elaborate

set of biomachinery.⁷⁻⁹ Although it has been established that iron-sulfur clusters of various stoichiometries will spontaneously assemble in vitro devoid of any proteinaceous assistance,^{10,11} the inherent toxicity of free iron and sulfur necessitates a dedicated biosynthetic complex by which these cytotoxic components can be safely incorporated into cofactors. The study of iron-sulfur cluster biogenesis is an endeavor over twenty years in the making, one with significant clinical interest—disruption of proper iron sulfur assembly or transfer can manifest as a multitude of disorders, most notably the neurodegenerative disorder Friederichs's ataxia.^{12,13} This motivation has driven tremendous research into the specifics of iron-sulfur cluster assembly across prokaryotic and eukaryotic organisms alike, with the former serving as a model system for the latter, which has established itself to be remarkably complex. Such an excursion into prokaryotic iron-sulfur cluster assembly is the basis for the project on which this thesis is predicated.

The investigation of iron-sulfur cluster biogenesis in prokaryotes has been a rigorous undertaking that has provided the field with critical insight into the nature of this process. Through these research endeavors, it has been determined that the assembly of a [2Fe-2S] cluster is accomplished through the liberation of sulfur from cysteine via the activity of a cysteine desulfurase, the incorporation of two irons from a yet to be determined iron-donor, and the addition of two electrons from a redox source that may or not be proteinaceous.^{6,8,14-17} The identification of three major operons involved in iron-sulfur cluster biosynthesis has paved the way for more detailed inquiries into the manner in which these cofactors are assembled. These three operons, ISC, SUF, and NIF, encode genes responsible for the components of the biomachinery for iron-sulfur cluster synthesis.^{6,17-19} In many prokaryotes, such as *E. coli*, the ISC system is the predominant means of basal iron-sulfur cluster assembly,^{16-18, 20-22} whereas the

SUF system is used to produce iron-sulfur clusters under oxidative stress conditions.^{16,17,22,23} Together, these two systems are responsible for the synthesis of nearly all of the iron-sulfur clusters present in the cell. The third system, NIF, is found in nitrogen fixing bacteria, and is involved primarily in the assembly of the iron-sulfur cluster that is incorporated into nitrogenase.^{17,19,21,22} The ISC system has generated the most interest out of the three aforementioned operons, in part due to erroneous assumption of its status as the ancestral system. This school of thought was fostered due to its conservation in the mitochondrial iron-sulfur assembly of eukaryotes, a consequence of endosymbiosis. However, further study has since ameliorated the field's view, as it is currently believed that the SUF system is the true archetypal system for iron-sulfur cluster assembly, with a greater scope across organisms than the ISC.⁴ Nevertheless, as a result of the bulk of iron-sulfur cluster biogenesis research conducted primarily on *E.coli*, *S. cerevisiae*, and humans, the ISC system has retained high research interest, and will serve as the primary focus of the work presented in this thesis.

The ISC operon, depicted in Figure 1-2²⁴ is a cluster of 8 genes proposed to be primarily

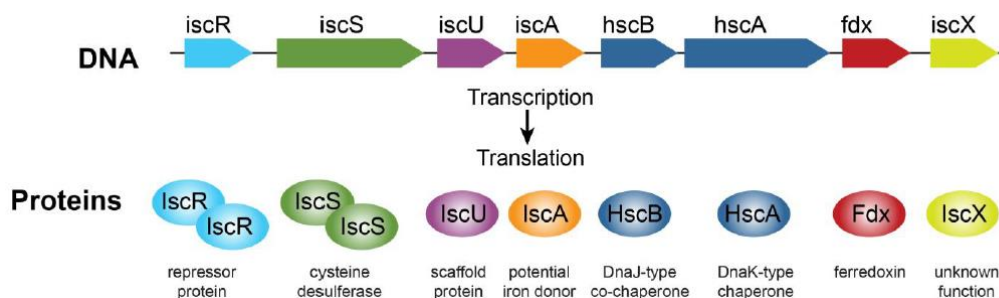
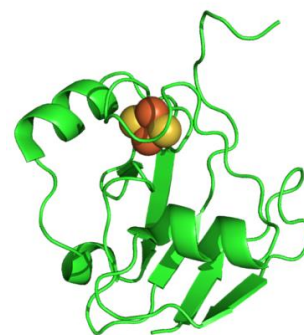


Figure 1-2. Depiction of the ISC operon in *E. coli*. Reprinted with permission from *Biochim. Biophys. Acta Mol. Cell Res.* 2015, 1853 (6), 1416–1428. Copyright © 2014 Published by Elsevier B.V.

involved in the assembly and transfer of [2Fe-2S] and [4Fe-4S] clusters. Depletion of the proteins encoded by this operon has been shown to attenuate the development of mature iron-

sulfur cluster proteins, evidenced by the findings of the Takahashi group.^{8,9,25} The expression of this operon is controlled by the first gene encoded, the transcription factor IscR. Under conditions in which iron-sulfur cluster assembly is plentiful (iron replete conditions), IscR will ligate a [2Fe-2S] cluster and act as a repressor for the operon to quell any further iron-sulfur cluster assembly.^{26,27} However, under conditions that fail to promote formation of holo-IscR, such as oxidative stress or iron starvation, the apo-protein will then activate expression of the ISC operon to stimulate iron-sulfur cluster biosynthesis.^{26,28-30} The initial process for [2Fe-2S] synthesis is achieved through the functionality of the remainder of the genes in the operon—the cysteine desulfurase IscS which through a PLP mediated mechanism catalyzes the conversion of cysteine into alanine, generating a persulfide on its mobile S-transfer loop cysteine to provide the source of sulfur,^{7,17,31} the scaffold protein IscU which houses the nascent clusters,^{7,16,17} the A-type carrier IscA that can transfer [2Fe-2S] clusters and may serve as an iron donor,^{17,32-34} the chaperone proteins HscA and HscB, which utilize ATP to possibly transfer newly formed clusters to other acceptor proteins,³⁵⁻³⁸ a [2Fe-2S] adrenoredoxin-like ferredoxin Fdx that has been proposed to serve as the source of electrons required for [2Fe-2S] biosynthesis,^{17,39-42} and finally, IscX, a small acidic protein speculated to be an iron donor.^{9,43-46} It is proposed that in the prokaryotic ISC system, an assembly complex for iron-sulfur cluster synthesis is comprised of the IscS homodimer, the IscU scaffold, with a series of accessory proteins that may bind and release depending on their function.^{6,15-17,22,47-50} The extent to which the members of the ISC operon have been characterized is highly variable—IscR, IscS, and IscU are well defined in both their structure and function, where by contrast IscA, Fdx, IscX, and HscA/B still carry lingering questions regarding their functionality, despite the insight already gleaned into their individual structures.

One of the aforementioned proteins of the ISC operon that warrants additional study is the adrenoredoxin-like ferredoxin Fdx, depicted in Figure 1-3⁴⁹. This small, acidic protein stably ligates a [2Fe-2S] cluster through four cysteine residues—Cys42, Cys48, Cys51, and Cys87.^{49–53} This cluster exists in two oxidation states, +1 and +2; with a reported redox potential of -380 mV,^{49,52,54} Fdx can perform one electron chemistry, akin to other globular ferredoxins, and receives its electron from the flavoprotein ferredoxin



PDB: 1i7h

Figure 1-3. Crystal structure of *E. coli* Fdx with its [2Fe-2S] cluster bound.

NADP reductase.^{38,49,54,55} Given its presence in the ISC operon, it is considered to be the putative electron donor for [2Fe-2S] and possibly even [4Fe-4S] assembly,⁵⁶ with the former more probable. While its precise function remains elusive, Fdx does not display behavior consistent with other ferredoxins. Earlier studies conducted upon its initial discovery determined that it could not supplant putidaredoxin in p450 mediated camphor hydrolysis, nor facilitate NADP photoreduction in the manner of plant ferredoxins.^{17,38,49–52} Failure to participate in reactions akin to other ferredoxins suggests a unique, uncharacterized niche for Fdx. Fitting with this hypothesis, there are established studies that confirm its necessity for overall iron-sulfur cluster biosynthesis—knocking down Fdx in *E.coli* demonstrates perturbations in the quantity of mature iron-sulfur cluster proteins.^{5,7-9} However, there are several conundrums worth discussing that arise from employing Fdx as the physiological reductant, chief of which is the somewhat paradoxical nature of employing a protein with a [2Fe-2S] cluster in order to synthesize [2Fe-2S] clusters. This situation suggests that a Fdx-independent pathway for assembling [2Fe-2S] clusters exists, but the reductant for such a system is unknown, with no other possible redox

protein even proposed to fulfill this task. It may be possible that a secondary system might even be the SUF pathway, which is not thought to require a ferredoxin-like protein as a reductant. Another incongruity is the necessity of two electrons for [2Fe-2S] cluster assembly, which clashes with Fdx's behavior as a single electron donor. This suggests either that an oxidized Fdx needs to be replaced by a new, reduced Fdx in the assembly complex, or that the presence of co-reductant (like a flavin, for example) is necessary for [2Fe-2S] cluster biosynthesis. However, at the current moment, such choreography involving different Fdx species has never been observed, and a structure of Fdx on the assembly complex itself has never been determined, only proposed through models constructed from NMR and SAXS data.⁵⁷

The current consensus on ISC pathway mediated [2Fe-2S] assembly, both prokaryotic and eukaryotic, considers the physiological reductant for this process to be the [2Fe-2S] ferredoxin, be it Fdx in *E.coli*, Yah1 in *S. cerevisiae*,^{38,58-60} and FDX2 in humans^{41,61-63}. The support for this premise has solid backing *in vivo*—deletions or knockdowns of this protein and its homologues have consistently demonstrated defects in growth and the capacity of the organism to properly assemble iron-sulfur clusters, evident in the attenuated activity of iron-sulfur cluster proteins such as succinate dehydrogenase.^{8,38,60,-64} Unique to eukaryotic systems, [2Fe-2S] ferredoxin deletions manifest as a mitochondrial iron accumulation phenotype. In humans, the inability to properly express FDX2 manifests as mitochondrial myopathy, with severe defects in the respiratory complexes and aconitase activities, all of which bear iron-sulfur clusters.^{65,66} While it is evident that Fdx plays an indispensable role in the proper assembly of iron-sulfur clusters, its precise function has yet to be elucidated. *In vitro* assays have been conducted in attempts to ascertain the function of Fdx in [2Fe-2S] assembly, but conclusive results have been minimal. A contributing factor to the gap in knowledge surrounding Fdx is the utilization of artificial

reductants in many of these *in vitro* assays.^{14,16-18,30,36,68,74} Studies of [2Fe-2S] cluster assembly with IscS and IscU have often opted to use artificial reductants such as DTT or small molecule thiols such as glutathione, and while these assays were instrumental in clarifying the functions of those components of iron-sulfur cluster biogenesis, they failed to account for a physiological source of reducing equivalents. This oversight has subsequently resulted in a lag in the understanding of Fdx compared to the other members of the iron-sulfur cluster assembly complex. If the goal of investigating the ISC system is to uncover the physiological mechanism in which iron-sulfur clusters are assembled, it is prudent to include Fdx and the corresponding ferredoxin NADP reductase to ensure biological relevance. Unfortunately, such studies have been uncommon, with the few incorporating this natural reducing system grappling with the fact that cluster synthesis is hampered *in vitro* comparatively to DTT mediated reactions.^{40,55} Nevertheless, it is an endeavor that necessitates additional investigation. By uncovering the precise function of the [2Fe-2S] ferredoxin in the simpler *E. coli* ISC system, a stepping stone is provided towards the elucidation of the physiological role of [2Fe-2S] ferredoxins in more complex eukaryotic systems.

The body of work concerning the *E. coli* Fdx (along with its eukaryotic homologues) and its role in [2Fe-2S] assembly has uncovered several facets of its behavior, especially in context with its association with the cysteine desulfurase IscS. The interaction between these two proteins has been previously established by means of co-purification studies.^{9,15} This association was then further characterized through SOFAST HMQC and 2D ¹H-¹⁵N HSQC NMR, performed by the Pastore laboratory, where it was determined that IscS exhibited stronger affinity for Fdx that bore a [2Fe-2S] cluster compared to the apoprotein.⁵⁷ The region in which Fdx signals were perturbed the most corresponded with residues adjacent to the [2Fe-2S] cluster, viewable in

Figure 1-4.⁵⁷ With the holoprotein, this same lab conducted BLI studies that determined the dissociation constant for the Fdx-IscS interaction to be $1.5 \pm 0.4 \mu\text{M}$, which is remarkably similar to that seen between IscS and IscU ($1.5 \pm 0.3 \mu\text{M}$).⁵⁷ With such a tight interaction, it can be presumed that this binding event between Fdx and IscS is significant, and can be relevant in the context of iron-sulfur cluster assembly. The nature of this interaction was further explored through additional NMR spectroscopy and mutagenesis, which located an acidic patch on Fdx consisting of

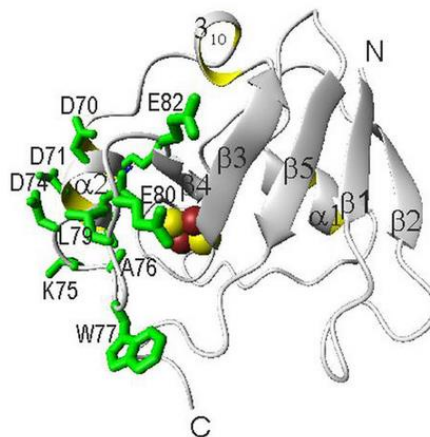


Figure 1-4. Structure of holo-Fdx, residues highlighted in green exhibit the greatest extent of perturbation seen in NMR when IscS is present. Adapted from *J. Biol. Chem.* 2013, 288 (34), 24777–24787.

residues 68-80 (primarily glutamates and aspartates) that was found to interact with a positively charged region on IscS.⁵⁷ Mutations of these charged residues abolished the binding event, confirming their necessity in facilitating the interaction. Incorporation of an *in vivo* assay affirmed that perturbing the Fdx-IscS interaction attenuates iron-sulfur cluster synthesis, evident in the lack of a [2Fe-2S] cluster ligated to the transcription factor IscR and the subsequent expression of a gene fused to a reporter. The proposed model of the Fdx-IscS complex, developed through NMR and SAXS data, depicted in Figure 1-5,⁵⁷ features two Fdx monomers bound on opposite sides of the IscS dimer interface, suggestive of the [2Fe-2S] cluster on Fdx oriented in a manner consistent with electron donation to the active site. As suggested previously, the nature of the interaction between Fdx and IscS is primarily electrostatic, with the charged regions germane to the binding region highlighted in

Figure 1-5.⁵⁷ This region on IscS that houses Fdx is also suggested to be the area in which the bacterial frataxin CyaY binds, which lends itself to the notion that Fdx and CyaY may compete for access to IscS. The

forementioned model suggests the existence of a hypothetical ternary

complex that features Fdx-IscS-IscU, visualized in Figure 1-6.⁵⁷ Such a complex has never been observed *in vitro*, and it remains unknown whether Fdx and IscU compete for binding on IscS, as this is a point of contention in the literature.

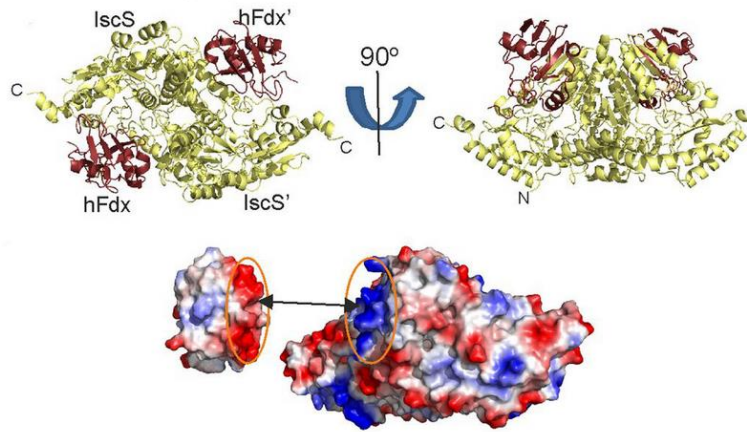


Figure 1-5. Top, proposed HADDOCK model of a Fdx-IscS complex. Bottom, electrostatic potential map of the Fdx-IscS binding region. Adapted from *J. Biol. Chem.* 2013, 288 (34), 24777–24787.

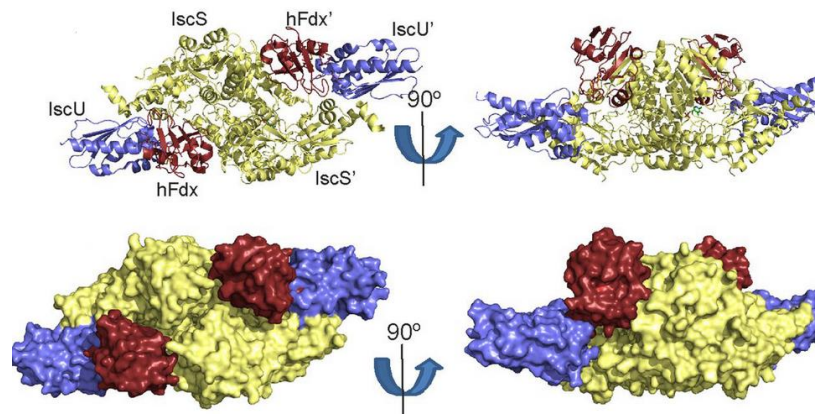


Figure 1-6. Proposed HADDOCK model of a hypothetical ternary complex of Fdx-IscS-IscU. Adapted from *J. Biol. Chem.* 2013, 288 (34), 24777–24787.

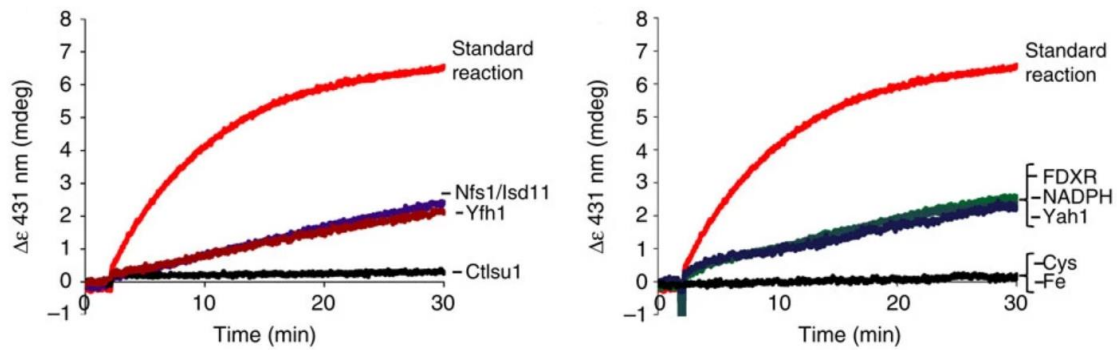


Figure 1-7. Time resolved circular dichroism spectroscopy of the formation of holo-Isu1. Elimination of Yah1 and its reductase attenuate the extent of [2Fe-2S] synthesis. Reprinted with permission from Springer Nature [Nature Communications] [Nat. Commun. 5:5013.] Copyright 2014 Springer Nature.

A key set of *in vitro* experiments to further cement the necessity of [2Fe-2S] ferredoxin for iron-sulfur cluster assembly was performed by the Roland Lill laboratory in *S. cerevisiae*, seen in Webert et al., 2014. These studies conducted were able to quantify the rate of [2Fe-2S] assembly on the scaffold protein Isu1⁴⁰. Time-resolved circular dichroism spectroscopic assays examined the incidence of [2Fe-2S] cluster formation on Isu1 under various conditions, gauging the effect the presence or absence of the yeast mitochondrial [2Fe-2S] ferredoxin Yah1, a homologue of Fdx. By monitoring the change of the wavelength that corresponds to holo-Isu1 over time in Figure 1-7,⁴⁰ it was determined that cluster assembly was dependent on the inclusion of Yah1 and a corresponding ferredoxin NADP reductase in reactions that already contains cysteine desulfurase (Nsf1), scaffold Isu1, L-cysteine, and ferrous iron. Under the same reaction conditions, with the exclusion of Yah1 and its reductase, no appreciable cluster formation on Isu1 was observed, implicating the ferredoxin as a prerequisite for cluster synthesis.⁴⁰ While these results are quite exciting in establishing the role of [2Fe-2S] ferredoxin in *de novo* cluster synthesis, there are some potential shortfalls to these experiments. These assays were conducted

using proteins from several different species—while the Yah1 and Nsf1 proteins were native to *S. cerevisiae*, the Isu1 originates from the thermophilic fungus *Chaetomium thermophilum*, and the ferredoxin NADPH reductase was not yeast Arh1, but rather the human homologue FDXR. Mixing species is a generally unfavorable practice, as the interactions that transpire in such assays are not necessarily reflective of the physiological reality in a single organism. Another issue that may have harmed the integrity of these assays is the inclusion of sodium ascorbate, a potential reductant, in the buffer systems. The presence of the ascorbate as a buffering agent casts doubt on whether the source of reducing equivalents for cluster synthesis came solely from the ferredoxin and its reductase. When coupled to a mixed-species assay, it becomes more difficult to accept the veracity of these findings.

The specific biochemical mechanism by which Fdx contributes to iron-sulfur cluster assembly has yet to be resolved, and this is still a significant gap in the established body of knowledge concerning the ISC system and eukaryotic iron-sulfur cluster biosynthesis. [2Fe-2S] ferredoxins such as Fdx perform one electron chemistry, and in the *de novo* biosynthesis of [2Fe-2S] clusters, two electrons are required, which creates a potential incongruity with using a one electron donor for a two electron process. In spite of this conundrum, evidence has been presented for the redox activity of Fdx and its eukaryotic homologues contributing to the assembly of [2Fe-2S] iron-sulfur clusters. The genetic evidence that implicates Fdx in [2Fe-2S] cluster assembly has already been discussed previously; this section will focus on the *in vitro* studies carried out that demonstrate the potential [2Fe-2S] ferredoxin dependence of *de novo* iron-sulfur cluster assembly. One of the most influential studies in the field regarding this facet of Fdx behavior originates from the lab of John Markley³⁹ in which UV-Vis spectroscopy was utilized to characterize Fdx redox activity with other members of the iron-sulfur cluster assembly

complex. The absorption spectrum of Fdx changes with respect to the oxidation state of the [2Fe-2S] cluster, with the oxidized form presenting a distinctive “double hump” at 414 and 456 nm. In the aforementioned

experiment, the addition of equimolar reduced Fdx to a reaction mixture of IscS and its substrate L-cysteine in 5 times excess resulted in the evolution of the oxidized spectrum of Fdx over the course of thirty minutes, depicted in Figure 1-8.³⁹ This experiment was then carried out once more with the

inclusion of the scaffold protein IscU and ferrous iron. The results were the same, in which the evolution of the oxidized Fdx spectrum was observed over time. The main conclusion drawn from these studies stressed the necessity of Fdx for iron-sulfur cluster assembly, with attention drawn to how the product of the IscS cysteine desulfurase reaction is the recipient of electrons from reduced Fdx.³⁹ This was established through a control in which reduced Fdx was added to an IscS mutant (C328S) incapable of performing the cysteine desulfurase reaction. Though potentially an overreach, these results were also held as definitive proof for the role of Fdx in [2Fe-2S] cluster assembly in *E.coli*, and have oft been cited as such. The same lab also repeated these experiments⁴¹ with both human mitochondrial ferredoxins FDX1 and FDX2 and were able

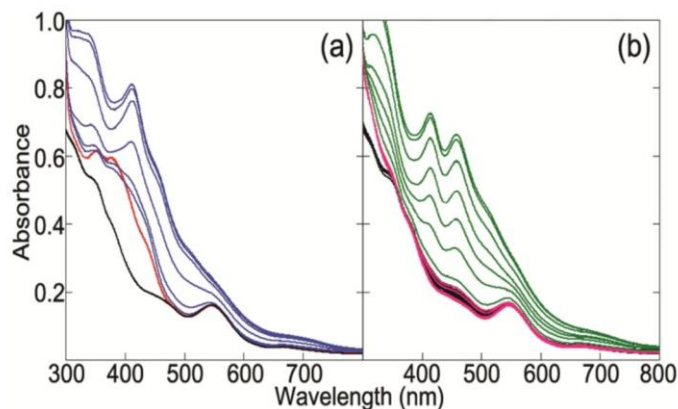


Figure 1-8. Time resolved UV-Visible spectra of (left) reduced Fdx, IscS, and cysteine, along with (right) reduced Fdx, IscS, IscU, cysteine, and Fe²⁺. The black traces represent the initial reduced Fdx. The blue and traces represent the spectra collected every 5 minutes over the course of 30 minutes post addition of L-cysteine. The green traces represent the spectra collected every 5 minutes for 1 hour post addition of L-cysteine. The red traces represent the spectra for reduced Fdx and IscS together in (a) and reduced Fdx, IscS, and IscU together in (b). Reprinted with permission from *J. Am. Chem. Soc.* 2013, 135, 8117–8120. Copyright 2013 American Chemical Society.

to observe the same results—reduced ferredoxin oxidizes in the presence of cysteine desulfurase and L-cysteine, as seen in Figure 1-9.⁴¹ The manner in which this phenomenon directly contributes to the assembly of [2Fe-2S] clusters was not addressed in a detailed manner in these works, though the overall conclusions drawn was that this redox activity of ferredoxin must contribute to cluster synthesis. Although these publications have significantly shaped the field’s view on the role of ferredoxin in iron-sulfur cluster biosynthesis, there are significant shortcomings with the experimental evidence presented. A considerable concern is the lack of data regarding the correlation of Fdx oxidation to holo-IscU formation, as UV-Vis spectroscopy is incapable of distinguishing the oxidized [2Fe-2S] on Fdx from [2Fe-2S] bound IscU. Therefore, the conclusion that iron-sulfur clusters were assembled on IscU due to the redox activity of Fdx is highly debatable; the integration of circular dichroism spectroscopy would have addressed this concern and establish without a doubt whether holo-IscU was generated from the given reaction mixture. The rate of the oxidation of the ferredoxin was

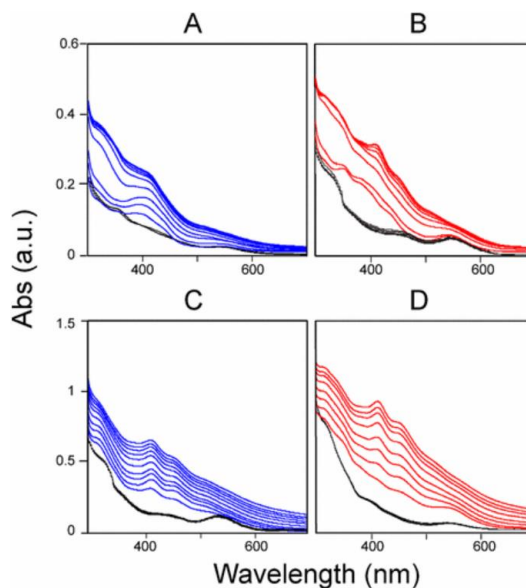


Figure 1-9. Time resolved UV-Visible spectra highlighting the change in oxidation state for FDX1 (A and C) and FDX2 (B and D). A and B represent the spectra of FDX1 and FDX2 respectively with cysteine desulfurase and L-cysteine. C and D represent the spectra of FDX1 and FDX2 respectively with the cysteine desulfurase, L-cysteine, the scaffold protein, and ferrous iron. The black traces represent the initial reduced FDX1 and FDX2. The blue traces represent the spectra collected every 5 minutes over the course of 30 minutes post addition of L-cysteine for A and B. The red traces represent the spectra collected every 5 minutes for 50 minutes post addition of L-cysteine for C and D. Reprinted with permission from *Biochemistry* 2017, 56, 487–499. Copyright 2017 American Chemical Society.

never quantified or examined more deeply so as to gauge whether the phenomenon is catalytically competent in the context of physiologically relevant iron-sulfur cluster assembly.

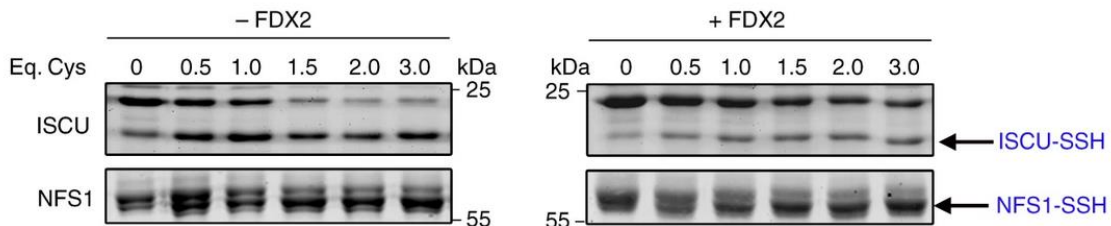


Figure 1-10. Persulfidation assay conducted with NFS1 and ISCU2 in the presence of reduced FDX2. Persulfidated NFS1 and ISCU2 were identified through a maleimide peptide assay. The persulfidated proteins were isolated and collected for further analysis. Presented here are SDS PAGE gels that depict the presence of persulfides on NFS1 and ISCU2, as indicated by the arrows. The gels displayed indicate conditions both with and without reduced FDX2. Only the persulfide on ISCU2, not NFS1, was reduced by FDX2. Adapted from *Nat Commun* 10, 3566 (2019).

The mechanism proposed by the Markley group in another publication suggested that Fdx reduces the persulfide on IscS to create a persulfide anion radical,⁴³ the existence of which has never been proven, let alone tested.

A competing theory, proposed more recently in 2019,⁶⁷ suggests that the ferredoxin reduction target is the persulfide generated on the scaffold protein following the cysteine desulfurase reaction. A persulfidation assay was conducted with the human mitochondrial iron-sulfur cluster assembly system to gauge whether the persulfide generated on the cysteine desulfurase NFS1 or scaffold protein ISCU2 is reduced by the potential electron donor FDX2. In this experiment, a maleimide peptide assay was employed to screen for persulfides on NFS1 and ISCU2. The persulfidated proteins would react with the maleimide peptide, allowing for them to be alkylated and adopt a higher mass, facilitating their characterization. With the persulfidated NFS1 and ISCU2 easily visible from the maleimide peptide assay, reduced FDX2 was added to each

protein, with the components subsequently run on an SDS PAGE gel. The ensuing results indicate that reduced FDX2 demonstrably reduces the persulfide on ISCU2, but not the persulfide situated on NSF1, depicted in Figure 1-10.⁶⁷ The ISCU2 in question had a ferrous iron bound—ISCU2 lacking in Fe²⁺ did not display reduction by FDX2 nor was it able to house nascent [2Fe-2S] clusters.⁶⁷ Such a phenomenon is consistent with the “iron first” mechanism postulated for [2Fe-2S] cluster synthesis, though this theory stems from studies specifically conducted in *E.coli*.⁶⁸ While the aforementioned data presented possibly presents some of the most definitive evidence in assigning a role for [2Fe-2S] ferredoxin in the iron-sulfur cluster biosynthetic complex, there remain yet still more questions. One that comes to mind is whether the reduction event detected in the persulfidation is truly reminiscent of the physiological mechanism, or simply an *in vitro* occurrence. Past attempts to characterize the [2Fe-2S] cluster of Fdx have demonstrated that it cannot donate electrons for functions related to hydroxylation or photosynthesis,^{50,51} but the exact specificity the cluster possesses in shuttling electrons to targets is unknown, hence, the need for *in vivo* confirmation in order to properly assess a biological mechanism from *in vitro* results. Another matter to address regards the circular dichroism and UV-Vis spectroscopy assays conducted, as they were processed in a manner to entirely remove contribution from FDX2, which is a necessity in order to properly ascertain formation of holo-ISCU. Unfortunately, this practice subsequently precludes any potential inquiry into correlating the change in the oxidation state of FDX2 to holo-ISCU formation, a still unaddressed facet of its behavior in the biological synthesis of iron-sulfur clusters.

In regard to discerning the identity of the physiological reductant, it would be remiss to not discuss the potential role played by the biological antioxidant glutathione. This tripeptide is present in eukaryotes, as well as some bacteria and archaea. In bacteria such as *E. coli*,

glutathione can be found at concentrations up to 10 mM, a sign of its overall importance to cellular health.^{75,76} In addition to protecting the cell with antioxidant activity, glutathione has been implicated in iron metabolism. One such role of glutathione in this cellular network is to ligate iron-sulfur clusters on conjunction with CGFS class two glutaredoxins in cluster transfer reactions.⁷⁷ While glutathione is known to be essential for these later stages of iron-sulfur cluster assembly, there is controversy in regards to whether it plays a role earlier on in this process. Various *in vitro* iron-sulfur cluster synthesis assays have been conducted that incorporate glutathione as a reductant, and many have demonstrated that this tripeptide can supplant ferredoxin as a source of reducing equivalents. Whether this is physiologically relevant or yet another instance of exogenous reductants obfuscating the biological reaction is a question that has not been fully addressed and deserves additional insight. It may be possible that glutathione is a co-reductant with, or even a second option after ferredoxin.

Taken together, while there has been progress in the past two decades towards solving the mystery of iron-sulfur cluster assembly, a multitude of questions remain. The precise mechanism in which [2Fe-2S] clusters are fully synthesized has eluded researchers, an issue exacerbated by multitudes of *in vitro* studies conducted that omit ferredoxin outright and utilize artificial reductants. When taking into account studies that do incorporate [2Fe-2S] ferredoxin, the current understanding of this protein remains incomplete, with several major findings raising as many questions as they answer. It is the goal of this thesis to present additional insight into *E. coli* Fdx that has gone overlooked and warrants additional investigation.

2. SPECTROSCOPIC ANALYSIS OF ELECTRON TRANSFER IN *E. COLI* IRON-SULFUR CLUSTER ASSEMBLY

2.1. Introduction

The excursion into addressing the shortcomings surrounding *E. coli* Fdx research has primarily focused on delving deeper into experimental results that merit additional examination. Unfortunately, there is a limit to the research previously conducted with Fdx, as a more physiological reductant has proven to be unattractive in the general study of iron-sulfur cluster biogenesis—artificial reductants such as dithiothreitol (DTT) have cemented themselves as critical components of *in vitro* assays involving both iron-sulfur cluster synthesis and transfer, despite employment in the latter established as a potentially problematic practice.^{70–72} Even when considering those studies that do include Fdx, there is a lack of detailed analysis into its behavior, coupled with a tendency to put forth sweeping assumptions with little evidence. Granted, there are logistical challenges that accompany attempts to investigate Fdx—with a low reduction potential, preserving the reduced state of the protein proves to be quite challenging, even with adequate anaerobic operations. Over the course of this thesis, several of these hindrances will be discussed and how attempts were made to work around or circumvent them.

When perusing the established literature, the aforementioned Kim et al. 2013 has emerged as a primary source for the contemporary iron-sulfur cluster biogenesis field to ascribe a function for Fdx. Numerous publications in the past decade, ranging from reviews to novel research, have cited this work as irrefutable evidence for the role of Fdx as redox protein that acts in the initial phase of [2Fe-2S] cluster synthesis. However, as was addressed in the introduction, there are several fundamental ambiguities and questions surrounding this specific inquiry, that give pause into taking its assessment as gospel. It is these very deficiencies in which this project was

launched, in an attempt to determine whether or not this observed behavior of Fdx is truly in accordance with its physiological function.

The *in vitro* assays conducted by John Markley's lab have relied on Fdx that has had its [2Fe-2S] cluster reduced via artificial means, conditions that attempts in this laboratory have maintained. While the reductant of choice in those experiments was sodium dithionite, there have been significant setbacks in this laboratory in achieving consistent levels of [2Fe-2S] reduction using this reagent. A common occurrence was the removal of the [2Fe-2S] cluster outright from Fdx, even at the concentrations specified by other groups that have achieved reduction with sodium dithionite. To combat the difficulties encountered by utilizing such a reagent, an alternative reductant was found—titanium (III) citrate. This potent reductant has a reduction potential of -480 mV, strong enough to reduce the [2Fe-2] cluster of Fdx. The utilization of this reductant has proven to be quite successful, demonstrating consistent reduction of the [2Fe-2S] cluster on Fdx without any observable cluster loss. Throughout this thesis, titanium (III) citrate will be featured as the sole means of reducing Fdx, in part to more properly mimic other experiments, in part due to difficulties working with physiological ferredoxin NADP reductase, which for reasons unknown, was incapable of providing electrons to oxidized Fdx to change the [2Fe-2S] to its reduced state. The goal of these spectroscopic studies was to not only to attempt to confirm the aforementioned phenomena in this lab, but to expand upon the current understanding of *in vitro* Fdx behavior.

2.2. Experimental Procedures

Protein purification. *E. coli* IscS was cloned and expressed into a pET derived vector bearing a polyhistidine tag. The plasmids were subsequently transformed into *E. coli* Rosetta BL21 DE3 cells, which were grown in LB media at 37°C until the OD₆₀₀ reached 0.6. At this point, overexpression was induced via administration of 0.5 mM IPTG; the cells were grown into the night for an approximate total of 16 hours as the temperature was lowered to 16°C. The following morning, the cells were pelleted by centrifugation. The cells were lysed via sonication (Branson sonifier 450) into Buffer A (50 mM HEPES 500 mM NaCl 5 mM imidazole pH 7.5), centrifuged, with the supernatant collected and loaded onto a Ni-NTA column (GE Life Sciences). This material was eluted with a linear gradient of Buffer B (50 mM HEPES 250 mM NaCl 500 mM Imidazole pH 7.5) from 5 to 500 mM imidazole. The corresponding yellow fractions were collected, concentrated, and subsequently loaded onto a Sephacryl S300 size exclusion column (26/60, GE Healthcare) that had been equilibrated prior with 50 mM HEPES 250 mM NaCl pH 7.5. The ensuing yellow fractions were collected and concentrated before being flash frozen and stored at -80°C.

E. coli Fdx was cloned into a pET28a vector bearing His-GFP-TEV, cloned into the C-terminal side of TEV via MEGAWHOP40. This plasmid was then transformed into *E. coli* Rosetta DE3 cells and grown in LB media at 37°C until the OD₆₀₀ reached 0.6. At this point, the temperature was lowered to 25°C, and overexpression was induced with administration of 0.4 mM IPTG (Research Products International). To maximize the incidence of holo-Fdx, 0.1 mg/mL ferric ammonium citrate (Amresco) and 1 mM L-cysteine (Sigma Aldrich) were administered to the cultures, which were allowed to grow overnight at 25°C for approximately 16 hours. The following morning, the bright green cell pellets were harvested by means of centrifugation and

stored at -80°C until purification. Lysis of the cells was achieved by sonication (Branson sonifier 450) into Buffer A (50 mM HEPES 500 mM NaCl 5 mM imidazole pH 7.5), with centrifugation of the lysed material performed to collect the green-brown supernatant. This material was loaded onto a Ni-NTA column (GE Life Sciences) and eluted with a linear gradient of Buffer B (50 mM HEPES 250 mM NaCl 500 mM Imidazole pH 7.5) 5 to 500 mM imidazole. The corresponding green-brown fractions were obtained and concentrated to undergo overnight TEV cleavage into Buffer A (50 mM HEPES 500 mM NaCl 5 mM imidazole pH 7.5). The cleaved protein was run on a second Ni-NTA column, with the brown flowthrough collected, concentrated, and subsequently loaded onto a 27 mL anion exchange column (16 mm \times 13.5 cm, POROS HQ 50). The protein was eluted with a linear gradient up to 1 M NaCl, and the brown fractions were pooled and concentrated before loading onto a 26/60 Sephadex 100 size exclusion column (GE Life Sciences) equilibrated beforehand with 50 mM HEPES 250 mM NaCl pH 7.5. The brown, monomeric fractions were collected, concentrated, flash frozen, and stored at -80°C .

E. coli IscU was cloned into a pFN2K Flexi vector bearing a GST sequence with N-terminal polyhisitidine tag and corresponding TEV cleavage site. The plasmid was transformed into *E. coli* Rosetta DE3 BL21 cells and grown in LB media at 37°C until reaching an OD_{600} of 0.6. To promote better folding of the protein, $8.9\ \mu\text{M}$ zinc sulfide heptahydrate was added to the culture. When the desired OD_{600} had been reached, protein overexpression was induced by addition of 0.5 mM IPTG; the temperature was held at 37°C as the cells were allowed to grow for another 3.5 hours before the pellets were harvested by centrifugation. Lysis of the cells was carried out by sonication (Branson sonifier 450) into Buffer A (50 mM HEPES 500 mM NaCl 5 mM imidazole pH 7.5), with centrifugation of the lysed material performed to collect the supernatant. This material was loaded onto a Ni-NTA column (GE Life Sciences) and eluted with a linear

gradient of Buffer B (50 mM HEPES 250 mM NaCl 500 mM Imidazole pH 7.5) from 5 to 500 mM imidazole. The fractions were collected and concentrated for overnight dialysis into Buffer A to perform TEV cleavage. 1 mM DTT (Research Products International) and 0.5 mM EDTA (Research Products International) were added to the buffer to minimize disulfide bond formation and potential aggregation. The following morning, the cleaved protein was loaded onto a second Ni-NTA column, with the flowthrough collected and concentrated. The protein was administered DTT for a final concentration of 5 mM before being sealed into a super loop and brought into an anaerobic MBraun Labmaster SP glovebox (<1 ppm of O₂ monitored by a Teledyne model 310 analyzer), where it was loaded into a Sephacryl S300 size exclusion column (26/60, GE Healthcare) that had been equilibrated prior with 50 mM HEPES 250 mM NaCl pH 7.5. The fractions corresponding to monomeric IscU were collected and concentrated down before being flash frozen and stored at -80°.

E. coli Grx4 was cloned into a pET28a vector bearing His-GFP-TEV, cloned into the C-terminal side of TEV via MEGAWHOP40. This plasmid was then transformed into *E. coli* Rosetta DE3 cells and grown in LB media at 37°C until the OD₆₀₀ reached 0.6. At this point, the temperature was lowered to 25°C, and overexpression was induced with administration of 0.4 mM IPTG. To maximize the incidence of holo-Grx4, 0.1 mg/mL ferric ammonium citrate and 1 mM L-cysteine (added 30 minutes post L-cysteine) were administered to the cultures, which were allowed to grow overnight at 25°C for approximately 16 hours. The following morning, the bright green cell pellets were harvested by means of centrifugation. Lysis of the cells was achieved by sonication (Branson sonifier 450) into Buffer A (50 mM HEPES 500 mM NaCl 5 mM imidazole pH 7.5), with centrifugation of the lysed material performed to collect the green-brown supernatant. This material was loaded onto a Ni-NTA column (GE Life Sciences) and

eluted with a linear gradient of Buffer B (50 mM HEPES 250 mM NaCl 500 mM Imidazole pH 7.5) 5 to 500 mM imidazole. The corresponding green-brown fractions were obtained and concentrated to undergo overnight TEV cleavage into Buffer A (50 mM HEPES 500 mM NaCl 5 mM imidazole pH 7.5). The cleaved protein was run on a second Ni-NTA column, with the brown flowthrough collected, concentrated, and subsequently loaded onto a 27 mL anion exchange column (16 mm × 13.5 cm, POROS HQ 50). The protein was eluted with a linear gradient up to 1 M NaCl, and the brown fractions were pooled and concentrated before loading onto a 26/60 Sephadex 100 size exclusion column (GE Life Sciences) equilibrated beforehand with 50 mM HEPES 250 mM NaCl pH 7.5. The brown, monomeric fractions were collected, concentrated, flash frozen, and stored at -80°C.

Reduction of Fdx. Artificial reduction of Fdx was carried out through the use of titanium (III) citrate. This reductant was synthesized in house using a modified version of the protocol outlined by Seefeldt and Ensign.⁷² The fully synthesized titanium (III) citrate was stored in the MBraun anaerobic glovebox at all times to ensure no oxidation of Ti^{3+} to Ti^{4+} transpired. Reduction of Fdx was carried out through administration of 5 mM titanium (III) citrate; the mixture was allowed to incubate for 30 minutes, during which time a noticeable color change from brown to pink was observed. Excess reductant was removed by passing the reduced Fdx through spin desalting columns (Micro Bio-Spin P6 Gel Columns); Fdx oxidation state and absence of titanium (III) citrate were confirmed through UV-Visible spectroscopic determination prior to use in assays.

UV-Visible spectroscopic assays. Assays were performed by employing an Ocean Optics USB 2000+ UV-Visible spectrophotometer configured to be operational inside of an anaerobic MBraun

LabMaster SP glovebox. A quartz cuvette with 1 cm pathlength was kept inside the glovebox so as to be entirely anaerobic in order to safely house oxygen sensitive samples. All assays were conducted in Assay Buffer (50 mM HEPES 250 mM NaCl pH 7.5) and performed directly inside the aforementioned cuvette. UV-Visible spectrophotometer parameters were as follows: 3 ms integration time; 100 scans to average, boxcar width of 5. IscS was added to the buffer solution first to subtract its contribution to the spectrum. Reduced Fdx would be added next, followed by L-Cysteine to initiate the reaction. For assays in which preincubation of IscS and L-cysteine was required, the two components were added together in the cuvette and allowed to incubate for approximately 30 minutes prior to administration of reduced Fdx. Assays employing mutants of IscS (C328A and C110A/C170A) used material purified previously by Dr. Shachin Patra. Time resolved UV-Visible spectra were collected at 1 minute intervals for specified periods of time as indicated in the results section. Assays conducted in the presence of an alternative reductant to cleave nascent persulfides that formed on IscS utilized 2 mM TCEP (Gold Biotechnology).

UV-Visible spectroscopic data processing. Raw data collected from the spectrophotometer was adjusted for baseline fluctuations manually by subtracting the contribution at 850 nm from all other wavelengths. The corrected data was then plotted as a function of time, with Excel employed to characterize spectral features encompassing longer range of wavelengths. Data that examined changes at a singular wavelength (456 nm) were processed with Kaleidagraph software.

Circular dichroism spectroscopy assays. Assays were performed using a Applied Photophysics Chirscan spectrophotometer, courtesy of Dr. Tadhg Begley. A quartz cuvette with a 1 cm pathlength fitted with a rubber septum (Sigma-Aldrich) and Parafilm was employed to ensure

samples housed within remained entirely anaerobic. Iron-sulfur cluster assembly assays were conducted using 30 μM IscU, 2 μM IscS, 100 μM L-cysteine, and 250 μM Fe^{2+} in the form of ferrous ammonium sulfate hexahydrate (Sigma-Aldrich). To probe the contributions from Fdx, 10 μM and 60 μM of both reduced and oxidized Fdx were added to the aforementioned assay conditions. Assessment of glutathione (GSH) was achieved through incorporation of 10 mM GSH (Sigma Aldrich) to previously described iron-sulfur cluster assembly assays. In all cases, spectral blanks were collected prior to initiation of the reaction, which could confirm the redox state of the Fdx. Reactions were commenced via injection of cysteine (and GSH when applicable) by means of a gas tight syringe to pierce the rubber septum. Spectra were collected every two minutes for ~45 minutes total. Assembly of [2Fe-2S] clusters on IscU could be tracked by following emergence of a peak at 330 nm.

Circular dichroism Spectroscopy data processing. Raw data was processed through ProData Viewer that was packaged with the Applied Photophysics circular dichroism software. Blank spectra were subtracted from the collected spectra, and the resulting data was smoothed through a mathematical application from the ProData Viewer. Full spectra were plotted in Excel, with the contribution from the first spectrum subtracted from all others. Plots examining the ellipticity at a single wavelength were created in Kaledagraph.

Radical trapping experiments. To explore whether a postulated persulfide radical anion intermediate species was generated from the electron transfer from Fdx to IscS, assays were conducted in the presence of a radical trapping agent, DMPO (5,5-dimethyl-1-pyrroline-N-oxide) (Ambeed Inc.). 10 μM IscS C110A/C170A and 50 μM to 100 μM L-cysteine were incubated

together in Assay Buffer for 30 minutes. This mutant was employed to minimize any contributions from the other cysteines when screening for adducts. After this incubation period, 1 mM DMPO was added to the solution mixture, followed by 10 μ M reduced Fdx. The reaction was quenched after 30 minutes by passing the solution thrice through a 30 kDa cutoff membrane spin concentrator (Vivaspin), and performing subsequent buffer exchange into MS-grade buffer made with ammonium acetate (Sigma Aldrich) at pH 7.5. All materials that came into contact with the reaction mixture from this point and onwards were triply rinsed with LC-MS grade water. A secondary cleanup step was performed by passing the solution through a 10 kDa cutoff membrane spin concentrator (Vivaspin) thrice, buffer exchanging into MS-grade ammonium acetate pH 7.5. Clean samples were prepared for denaturing mass spectrometry through addition of 1% formic acid, and were injected into a Thermo Xcalibur 4.0 Ultra high mass range (UHMR) mass spectrometer. Resulting data was deconvoluted and analyzed through use of UniDec (version 4.4.1) software.

2.3. Results

UV-Visible spectroscopic analysis of the behavior of reduced Fdx. Experiments previously conducted in the Markley lab were performed with the goal to ascertain how the redox activity of Fdx contributed to *de novo* [2Fe-2S] cluster assembly. The results obtained from their research ventures have asserted that reduced Fdx exhibits characterizable oxidation when exposed to IscS and L-cysteine.³⁹ The Markley group subsequently interpreted this result as evidence that reduced ferredoxin is reducing the persulfide intermediate created on the cysteine desulfurase IscS to generate a radical anionic species.⁴³ This result remains controversial as additional experimental support for the generation of a radical species was not provided and the kinetic

competence of this reaction was not established. There is also concern that the potentially insufficiently anaerobic conditions might have led to oxidation of the ferredoxin, a problem often encountered with this protein.

To probe the veracity of the aforementioned result, this manner of experiment was repeated using a UV-Visible spectrometer located in an anaerobic glovebox maintained below 1 ppm O₂. Fdx was artificially reduced using titanium (III) citrate, a reductant found to behave more favorably than the sodium dithionite commonly employed for such purposes. The oxidation state of the protein was confirmed by checking its UV-Visible spectral pattern, which was consistent for a [2Fe-2S]⁺¹ cluster. In a quartz cuvette, 50 μM IscS was added to Assay Buffer; to this mixture, 50 μM final concentration reduced Fdx was administered, followed by 250 μM L-cysteine. The reaction was left to proceed for 30 minutes, with spectra collected every minute. Controls in which reduced Fdx was added to either IscS or cysteine alone were also carried out. The results demonstrate that indeed, reduced Fdx oxidized over time solely in the presence of IscS and its substrate, evidenced by the evolution of the spectral “double hump” at 414 nm and 456 nm that is specific to an oxidized [2Fe-2S] cluster on this protein (Figures 2-1 and 2-2).

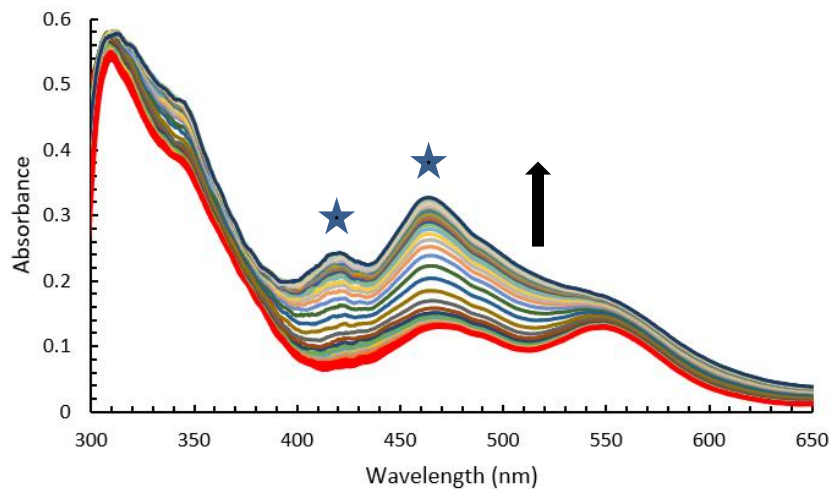


Figure 2-1. Time-resolved UV-Visible spectroscopy of 50 μM reduced Fdx, 50 μM IscS, and 250 μM L-cysteine over 30 minutes. Each trace represents the spectra collected at every minute. The initial spectrum of reduced Fdx ($t=0$) is indicated by the bottom red trace. The overall direction of the change in the spectra over time is indicated by the arrow, with the emergence of the “double hump” at 414 nm and 456 nm (noted by stars) characteristic of Fdx oxidation. Contribution from IscS was removed prior to collection of spectra.

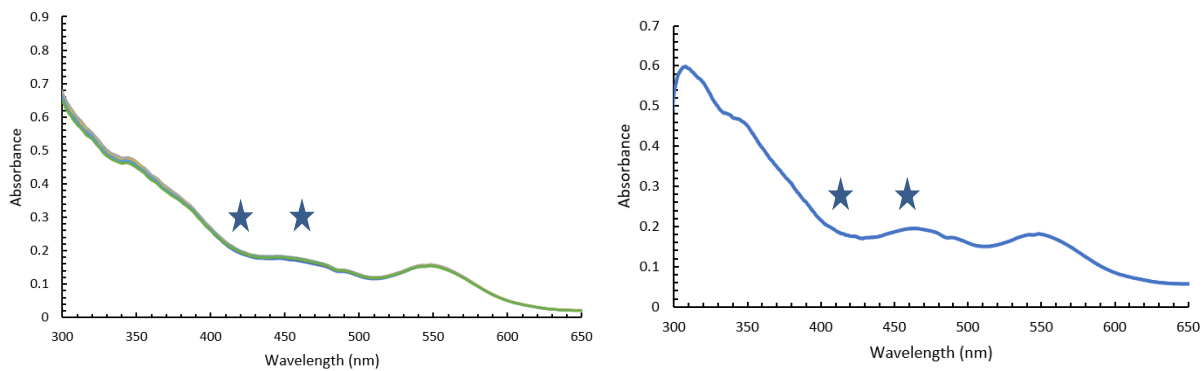


Figure 2-2. 50 μM reduced Fdx in the presence of 250 μM L-cysteine (left) and in the presence of 50 μM IscS (right). Spectra presented are the overlay of individual traces over 30 minutes. In these control experiments, the absence of peaks at 414 nm and 456 nm (noted by the stars) indicates that neither L-cysteine nor IscS alone are sufficient to oxidize Fdx.

Examination of the time dependent change in the spectra revealed that the oxidation of Fdx did not immediately occur upon the addition of L-cysteine, but rather, followed by a lag phase (Figure 2-3). A lag phase was reproducibly observed found for all trials conducted and appears to be a component of the reaction that was not addressed in the original literature.³⁹ To conserve protein stocks, the experiment was repeated, reducing the original concentrations down five-fold while maintaining the same ratios between reactants still displayed the exact phenomenon mentioned previously (Figures 2-4 and 2-5). The lag phase was determined to be approximately 10 minutes, unusual given how IscS can turnover cysteine 8.5 times per minute.⁷² From these results, it was tentatively proposed, in accordance with the established literature,³⁹ that reduced Fdx can donate electrons to the persulfide intermediate on IscS but not to either the cysteine substrate itself or the unmodified mobile S-transfer loop of IscS. However, the incidence of this

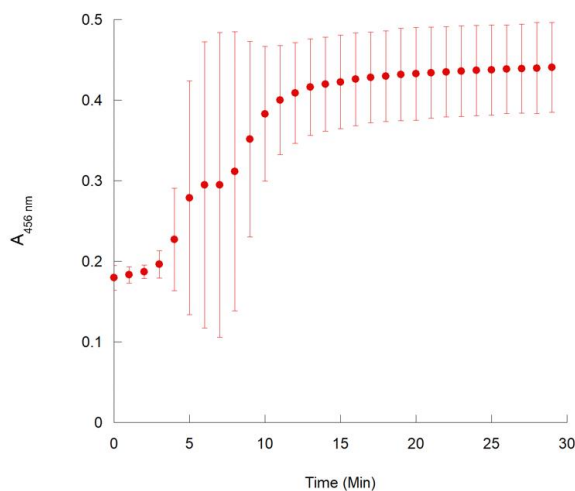


Figure 2-3. The change in absorbance at 456 nm monitored over the course of 30 minutes as a means of tracking the oxidation of Fdx. The plot was generated from the average of 3 experiments conducted in the manner of that seen in Figure 2-1. Note the delay in Fdx oxidation, the observable lag phase was found to average roughly 5 minutes for this set of experiments.

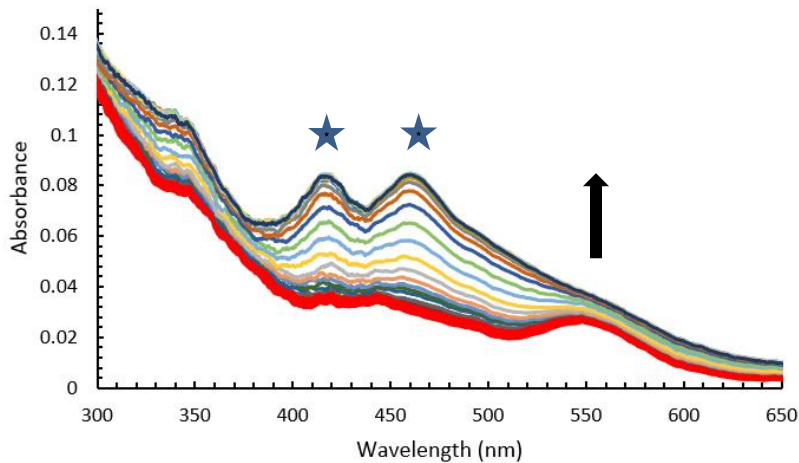


Figure 2-4. Time resolved UV-Visible spectroscopy of 10 μM reduced Fdx, 10 μM IscS, and 50 μM L-cysteine. Each trace represents the spectra collected at every minute. The initial spectrum of reduced Fdx ($t=0$) is indicated by the bottom red trace. The overall change in the spectra is indicated by the arrow, with the emergence of the “double hump” at 414 nm and 456 nm characteristic of Fdx oxidation (marked by stars). Contribution from IscS was removed prior to collection of spectra.

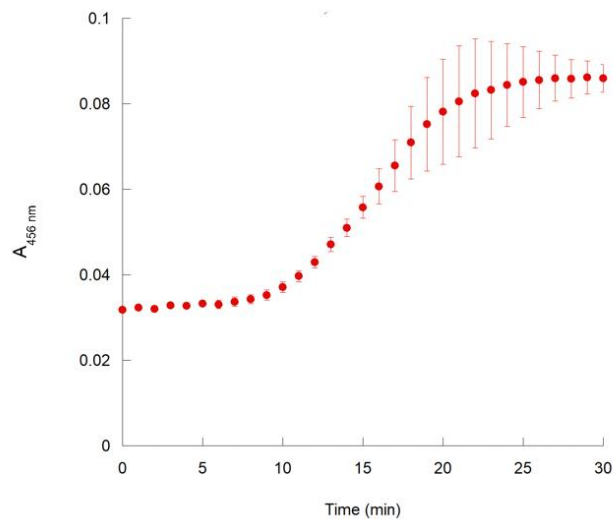


Figure 2-5. The change in absorbance at 456 nm monitored over the course of 30 minutes as a means of tracking the oxidation of Fdx. The plot was generated from the average of 3 experiments conducted in the manner of that seen in Figure 2-4. Note the delay in Fdx oxidation, the observable lag phase was found to average roughly 10 minutes for this set of experiments.

lag phase suggests that this reaction is not physiologically relevant in the actual assembly of ron-

sulfur clusters, as this time frame is not catalytically competent for cellular synthesis.

Isolating the target of Fdx electron transfer. To probe whether the oxidation of reduced Fdx was brought about solely by the persulfide generated on the catalytic cysteine of IscS (C328), different IscS mutants were employed—C328A, and the double mutant C110A/C170A. The former, bearing no catalytic cysteine, has no cysteine desulfurase activity; the latter only possesses the catalytic cysteine, limiting any potential side reactions. When 10 μ M reduced Fdx is incubated in the presence of 10 μ M IscS C328 and 50 μ M L-cysteine, the ensuing UV-Visible spectrum depicted no oxidation of Fdx, as would be expected if no cysteine desulfurase activity takes place (Figure 2-6). To further validate these results, UV-Visible spectroscopic assays were also conducted in the presence of 2 mM TCEP, a reductant known to cleave disulfide and persulfide linkages.⁷⁸ When oxidized Fdx is added to 2 mM TCEP, no reduction of the [2Fe-2S] cluster is observed, which confirms the selectivity of the reductant (Figure 2-7). If the cysteine desulfurase reaction between IscS and L-cysteine is allowed to proceed in the presence of TCEP, it is expected that any persulfides generated on C328 of IscS would be reduced by TCEP, leaving no target for electron transfer from Fdx. As expected, this is the very result that is observed (Figure 2-6). Repeating the experiment with 10 μ M IscS C110A/C170A revealed a similar oxidation of Fdx as seen with the native enzyme, demonstrating that only the mobile S-transfer loop cysteine is important for this phenomenon (Figure 2-8). However, it was noted that assays conducted with IscS C110A/C170A revealed a curious result—the time of the lag phase appeared to shorten when employing this mutant (Figure 2-9).

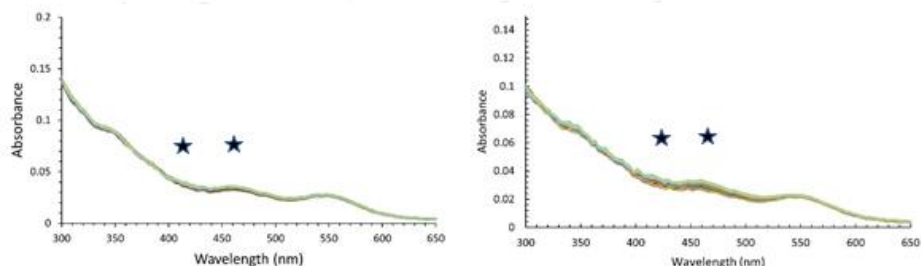


Figure 2-6. Time resolved UV-Visible Spectroscopy of 10 μM reduced Fdx, 10 μM IscS C328A, and 50 μM L-cysteine (left) and 10 μM reduced Fdx, 10 μM IscS, 50 μM L-cysteine, and 2 mM TCEP (right). Each trace represents the spectra collected at every minute. The lack of the characteristic double hump at 414 nm and 456 nm (marked by stars) signifies that under these conditions, Fdx was unable to oxidize. Contributions from IscS were removed prior to collection of spectra.

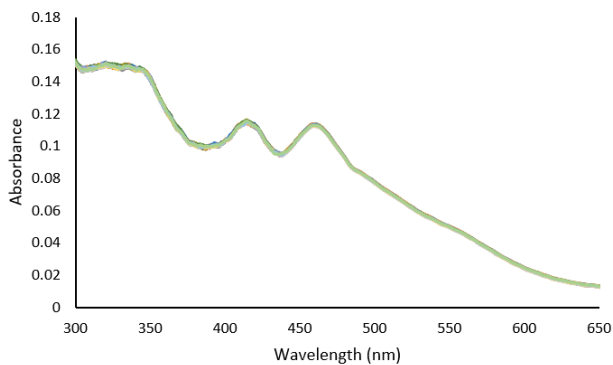


Figure 2-7. 10 μM oxidized Fdx in the presence of 2 mM TCEP. Spectra presented are the overlay of individual traces over 30 minutes. The persistence of the peaks at 414 nm and 456 nm indicates that TCEP is not a reductant capable of reducing Fdx.

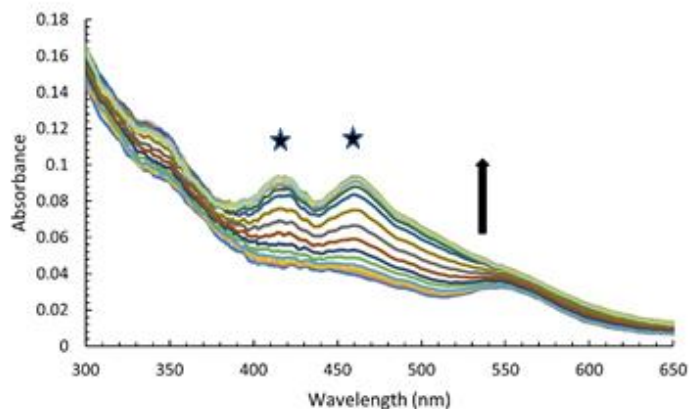


Figure 2-8. Time resolved UV-Visible spectroscopy of 10 μM reduced Fdx, 10 μM IscS C110A/C170A, and 50 μM L-cysteine. Each trace represents the spectra collected at every minute. The overall change in the spectra is indicated by the arrow, with the emergence of the “double hump” at 414 nm and 456 nm (marked by the stars) characteristic of Fdx oxidation, which is unaffected by the utilization of this mutant form of IscS. Contribution from IscS was removed prior to collection of spectra.

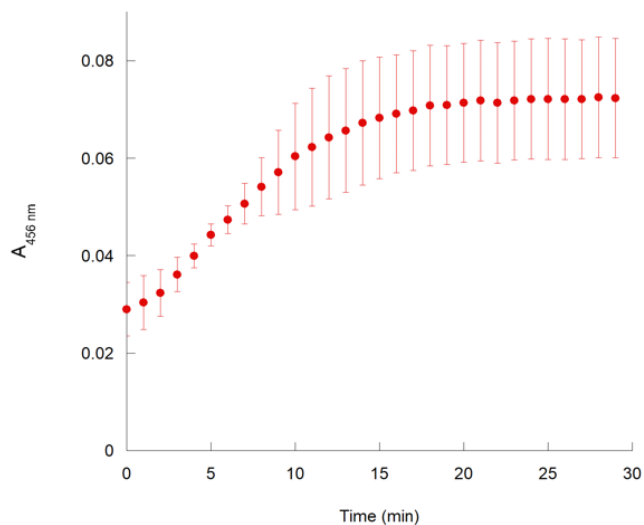


Figure 2-9. The change in absorbance at 456 nm monitored over the course of 30 minutes as a means of tracking the oxidation of Fdx. The plot was generated from the average of 3 experiments conducted in the manner of that seen in Figure 2-7. Note the lack of a considerable delay in Fdx oxidation, as it appeared to readily transpire under these conditions.

While these pieces of data establish the persulfide on IscS as a possible target of Fdx redox activity, they do not address another possibility—cysteine persulfide generated as a side product from L-cysteine mediated cleavage of the persulfide on IscS. It is possible that within the solution, some cysteine persulfide is formed as a byproduct of cysteine desulfurase activity, and this may also contribute to the global oxidation of Fdx witnessed in these assays. In order to discern whether this is in indeed a legitimate happenstance, a new set of assays were performed, in which 10 μ M IscS and various concentrations of cysteine were allowed to incubate together in Assay Buffer for 30 minutes. Following this passage of time, the solution was passed through a 100 kDa cutoff spin concentrator, (Vivaspin) where both the flowthrough and proteinaceous components were saved. A final concentration of 10 μ M reduced Fdx was added to each fraction, and the UV-Visible spectra were collected every minute for 30 minutes. The results show a stark contrast between the two experimental conditions (Figure 2-10). Proteinaceous persulfide—localized exclusively on IscS—readily oxidized Fdx, whereas the non-proteinaceous component demonstrated no conclusive effect on the oxidation state of Fdx. The lack of a lag phase seen with Fdx oxidation suggests that access to the persulfide on IscS is unabated under these conditions. Taken altogether, the findings presented in this section demonstrably rule out IscS residues C110A and C170A, along with postulated cysteine persulfide as contributors towards the oxidation event, leaving the persulfide formed on C328 as the primary target of electron transfer from Fdx in the context of this *in vitro* setting.

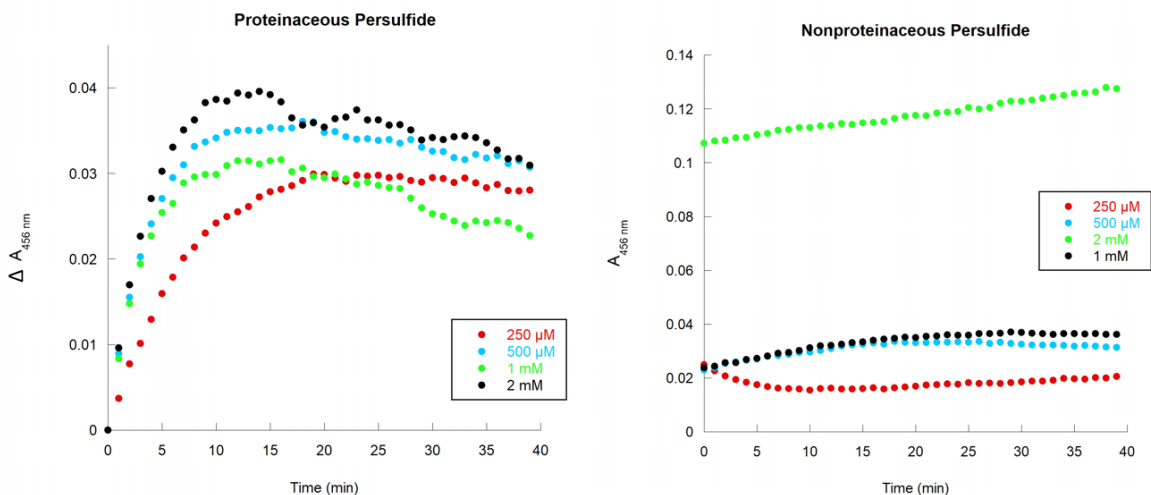


Figure 2-10. UV-Visible comparison of Fdx oxidation in the presence of proteinaceous persulfide and non-proteinaceous persulfide. Assays were conducted with 10 μM IscS and various concentrations of L-cysteine, which were preincubated together prior to separation with a spin concentrator. 10 μM reduced Fdx was added to the two separate components and examined with UV-Visible spectroscopy. The persulfide localized on IscS readily reduced Fdx, whereas the non-proteinaceous component failed to do the same. Traces followed the change at 456 nm and were the average of at least 2 or more experimental trials.

Modulating Cys concentrations and incubation times with IscS. The oxidation event observed with Fdx in this setting was further explored by varying the concentrations of L-cysteine administered in an attempt to discern whether this would change the length of the lag phase. The initial hypothesis revolved around the presumption that the lag phase was a consequence of low cysteine concentrations. To test this, trials were performed in which 250 μM , 500 μM , 1 mM, and 2 mM cysteine were added to the assay, maintaining the same concentrations of IscS and reduced Fdx. For each cysteine concentration, the change at 456 nm was plotted, and the amount of time elapsed before the absorbance at 456 nm begin to rise linearly was counted as the lag phase and averaged over triplicate trials. Unexpectedly, it was found that the greater the concentrations of cysteine, the longer the lag phase before Fdx oxidation (Figure 2-11). This unanticipated trend was consistent across repeated trials.

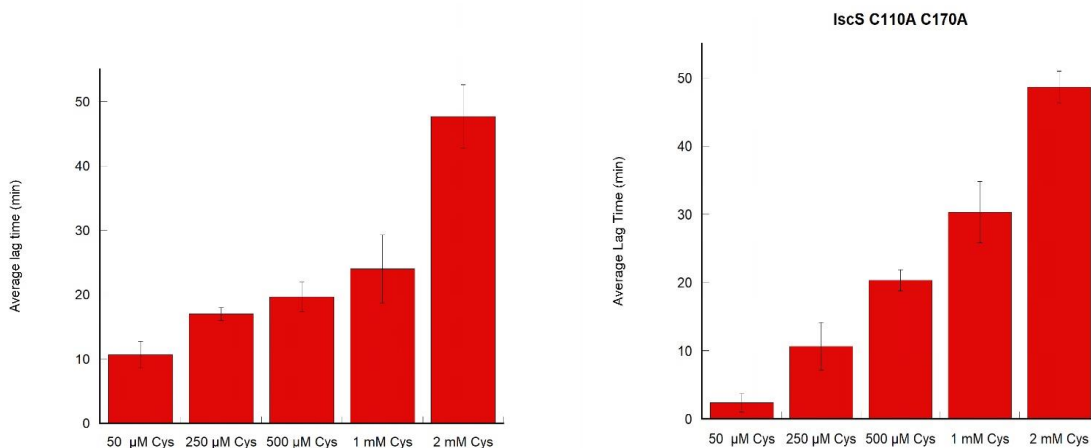


Figure 2-11. Comparison of average lag times before the advent of Fdx oxidation in UV-Visible assays conducted with 10 μ M reduced Fdx, 10 μ M IscS and various concentrations of L-cysteine. Left, lag times witnessed with WT IscS, right, lag times witnessed with C110A/C170A IscS. A consistent trend emerges in which greater concentrations of cysteine correlate with long lag phases before Fdx oxidation transpires. There was no discernable difference observed between studies conducted with WT IscS or the double mutant. Averages were taken from experiments conducted in triplicate.

In order to ascertain whether this lag phase was related to the presence of other cysteine residues on IscS, further assays were conducted in which 10 μ M reduced Fdx and variable concentrations of Cys were employed in the presence of 10 μ M IscS C110A/C170A. If the other cysteine residues were contributing in some manner to the lag phase of Fdx oxidation, employing the double mutant IscS in these assays would lead to an attenuation of this event. The results of these excursions do not substantiate the previously described hypothesis, and show no appreciable connection between the lag phase time and the form of IscS employed (Figure 2-11). Only the lowest Cys concentrations show a minor decrease in the overall lag phase time, but no such trend

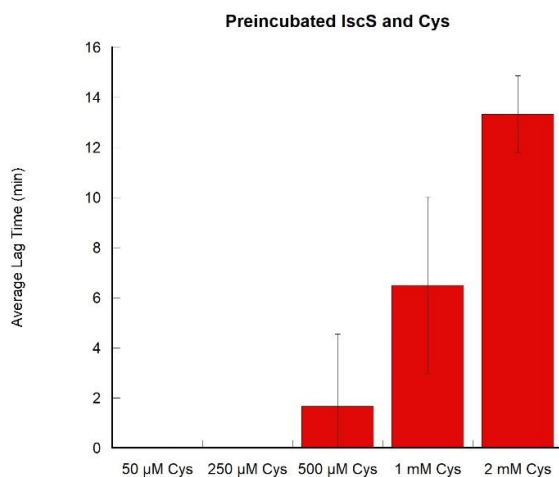


Figure 2-12. Comparison of average lag times before the advent of Fdx oxidation in UV-Visible assays conducted with 10 μ M IscS, and various concentrations of L-cysteine that had been incubated 30 minutes prior to the addition of 10 μ M reduced Fdx . Lag phases were found to attenuate or disappear entirely as a result of preincubation of IscS and cysteine. Averages were taken from experiments conducted in triplicate.

emerges further onwards, which raises doubts about the validity of these residues contributing to the lag phase in any meaningful capacity.

Another variable that was modified in these proceedings was the incubation time of IscS and its substrate. Previously, all aforementioned assays were conducted by adding IscS, reduced Fdx, and L-cysteine together and collecting spectra immediately following the addition of cysteine to initiate the reaction. To gauge whether the observed lag phase was perhaps related to an unexpected low turnover rate of the cysteine desulfurase, 10 μ M IscS and various concentrations (50 μ M – 2 mM) of L-cysteine were incubated together for 30 minutes prior to the addition of 10 μ M reduced Fdx. The ensuing results demonstrate that the lag phase was absent entirely at lower

concentrations, and greatly diminished at higher concentrations (Figure 2-12). The immediate conclusion is that with more time, the persulfide on IscS is allowed to develop to a capacity in which appreciable oxidation of Fdx can be observed spectroscopically, which is odd for an

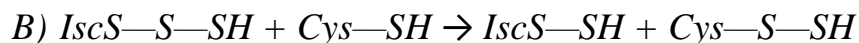


Figure 2-13. List of reactions at play in the assays conducted in Figures 2-1 to 2-12. A) is the cysteine desulfurase activity of IscS that removes the thiol group from cysteine to generate alanine, creating a persulfide on the catalytic cysteine of IscS. B) represents a potential side reaction between cysteine and IscS persulfide, in which cysteine behaves as a thiol reductant to cleave the persulfide on IscS. C) represents the interaction between IscS and reduced Fdx, in which Fdx reduces the persulfide on IscS. When cysteine is present in excess, it is possible that reaction B supplants reaction C, possibly explaining the lengthening lag phase of Fdx oxidation under these conditions.

enzyme that possesses the ability to turnover cysteine several times over the course of a minute.

Nevertheless, the results would indicate that the phenomenon described is most likely not catalytically competent and may not even be physiologically relevant in the context of biological iron-sulfur cluster assembly. It is likely that high concentrations of cysteine are creating competition for the persulfide on the catalytic cysteine of IscS, preventing reduced Fdx from transferring electrons to its target, such a model is proposed and outlined (Figure 2-13).

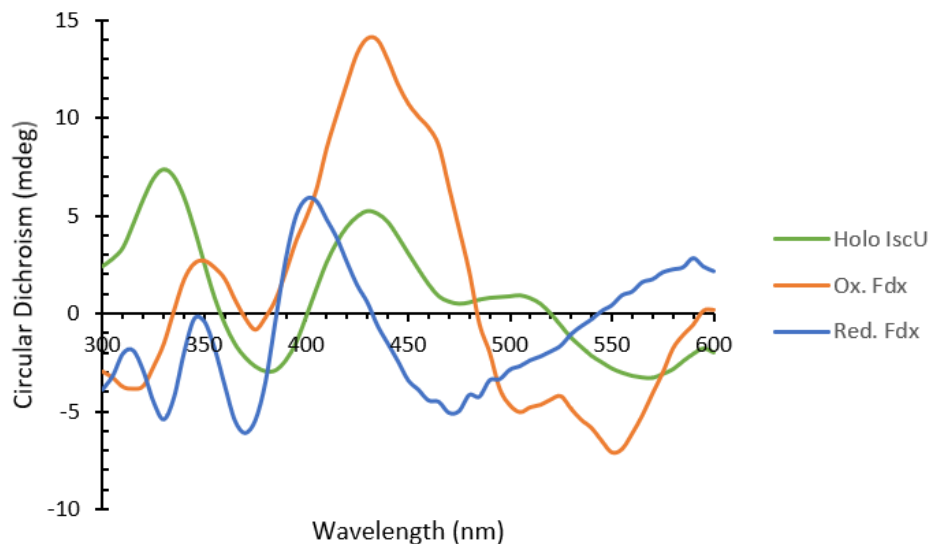


Figure 2-14. Circular dichroism spectra of holo-IscU, reduced Fdx, and oxidized Fdx. Holo-IscU formation is monitored at 330 nm, whereas oxidation of Fdx is observed through an increase in ellipticity in the region of 400-450 nm.

Examining the behavior of Fdx in iron-sulfur cluster assembly. To continue to delve into the behavior of Fdx, and to challenge the claims put forth in the Markley and Lill laboratories³⁹⁻⁴⁰, additional experiments were performed using circular dichroism spectroscopy, which could more reliably track iron-sulfur cluster formation on the scaffold protein IscU while simultaneously monitoring the redox activity of Fdx. This technique provides a unique advantage over UV-Visible spectroscopy, and can reliably differentiate [2Fe-2S] clusters built on the scaffold protein from the one already present in Fdx (Figure 2-14). To confirm that reduced Fdx is indeed necessary for iron-sulfur cluster assembly, assays were conducted in which 30 μ M IscU, 2 μ M IscS, 100 μ M L-cysteine, and 250 μ M ferrous iron were administered into a cuvette containing Assay Buffer. This mixture was prepared as described or with 10 μ M reduced Fdx, 10 μ M oxidized Fdx, 60 μ M reduced Fdx, or 60 μ M oxidized Fdx. Samples were run for 40 minutes, collecting spectra every 2 minutes. The change in circular dichroism was monitored at 330 nm,

the wavelength that corresponds to holo-IscU. By comparing the changes at this wavelength, one can probe which conditions best facilitate iron-sulfur cluster assembly. The results depict what

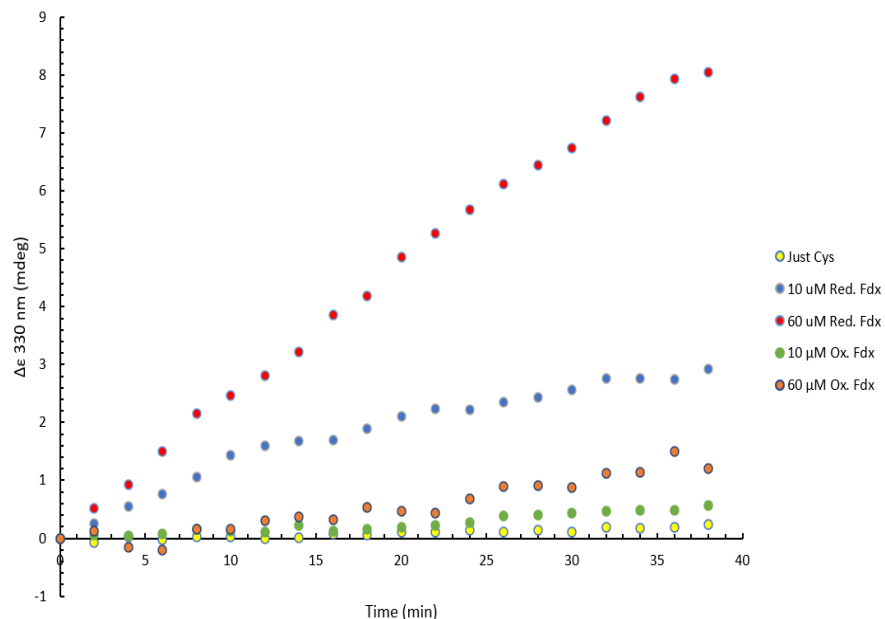


Figure 2-15. Time resolved circular dichroism spectroscopy of iron-sulfur cluster assembly on IscU. All reactions contained 30 μM IscU, 2 μM IscS, 100 μM L-cysteine, and 250 μM ferrous iron, with concentrations of reduced and oxidized Fdx varied. Formation of $[\text{2Fe-2S}]$ clusters was monitored via 330 nm, and the extent of cluster formation was found to be greatest under conditions with stoichiometric quantities of reduced Fdx.

one would expect, that the highest extent of iron-sulfur cluster assembly transpired in the presence of 60 μM reduced Fdx, stoichiometrically in line for a proposed one electron donor redox protein (Figure 2-15). This is not a finding of great surprise, as the *in vivo* evidence discussed in earlier in this work implicates Fdx as necessary for biological iron-sulfur cluster assembly. However, the major contribution of this assay is providing evidence that confirms the change in Fdx redox state during cluster synthesis. The global circular dichroism spectra collected from these assays seemingly indicates that as iron-sulfur clusters are assembled, the evolution of holo-IscU appears to coincide with the development of the oxidized Fdx spectrum.

As the 330 nm peak increases, so does the region from 400-450 nm. This finding has not been reported in the literature previously, and conclusively demonstrates the necessity of reduced Fdx specifically to facilitate iron-sulfur cluster assembly.

Examining the role of glutathione in iron-sulfur cluster assembly. While a major focus of this work has been to elucidate the role of the redox protein Fdx in biological iron-sulfur cluster assembly, it would be remiss to ignore another potential biological reductant, glutathione (GSH). This antioxidant is abundant in the cell—found in millimolar concentrations—and is known to play roles in downstream iron-sulfur cluster assembly by aiding glutaredoxins to coordinate iron-sulfur clusters during transfer events. In the context of [2Fe-2S] cluster assembly, whether GSH directly participates as a reductant remains unknown, but given its extensive presence in the cell, the possibility exists that it may be involved earlier in iron-sulfur cluster maturation than postulated. To assess such a possibility, circular dichroism assays were repeated, with 10 mM GSH incorporated into previously stated conditions that did and did not contain reduced Fdx. The results of these experiments demonstrate that GSH has a greater ability to promote initial iron-sulfur cluster assembly on IscU than reduced Fdx alone (Figure 2-16). The trace corresponding to 10 mM GSH shows a faster initial rate of iron-sulfur cluster assembly than even stoichiometric quantities of reduced Fdx. However, when reduced Fdx and GSH are both present within the same assay, the extent of iron-sulfur clusters produced on IscU was only slightly magnified. It would appear that the two reductants might complement each other, or at least have a small additive effect on each other in this *in vitro* setting. However, this is most evident when low concentrations of Fdx are incorporated into assays containing 10 mM GSH. Yet, there appears to be some conflicting behavior when GSH is added with higher

concentrations of Fdx, as there are overall lower quantities of [2Fe-2S] clusters assembled with 30 and 60 μM Fdx. Such findings lead to additional questions into the role of GSH in this

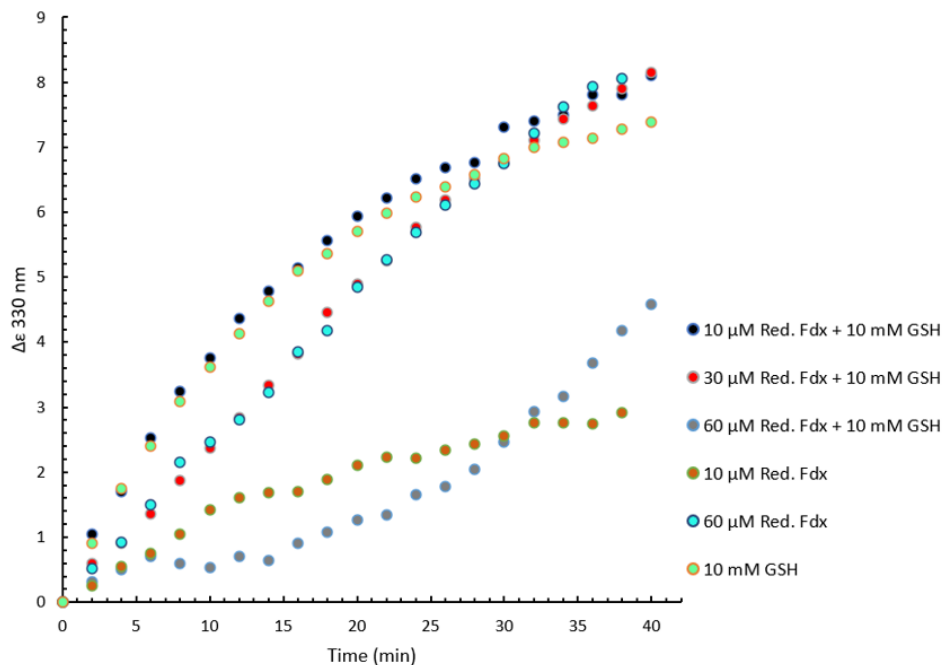


Figure 2-16. Time resolved circular dichroism spectroscopy of iron-sulfur cluster assembly on IscU. All reactions contained 30 μM IscU, 2 μM IscS, 100 μM L-cysteine, and 250 μM ferrous iron, with variations in the concentrations of reduced Fdx, and/or 2 mM GSH. Formation of [2Fe-2S] clusters was monitored via 330 nm, and the extent of cluster formation was found to be greatest under conditions with both GSH and reduced Fdx. However, GSH alone was found to facilitate iron-sulfur cluster assembly to a greater degree than reduced Fdx alone.

process, as it is not clear why the proposed physiological reductant, Fdx, is not as potent as a small molecule thiol alone in promoting iron-sulfur cluster assembly. Another facet of GSH involvement that was investigated was whether an entire cluster turnover event onto the carrier protein Grx4 could be accomplished in the presence of GSH. Circular dichroism, with its ability to distinguish between [2Fe-2S] clusters in different chiral environments, is capable of detecting a conversion from holo-IscU to holo-Grx4 over time. One concern that motivated this

experiment was the possibility that the previously performed iron-sulfur cluster assembly assays may have been producing immature [2Fe-2S] clusters—species that were still tethered to IscU by a disulfide linkage. To ensure that what has been viewed with GSH is a legitimate contributor to the development of mature [2Fe-2S] clusters, assays were performed with 30 μ M IscU, 2 μ M IscS, 30 μ M Grx4, 100 μ M L-cysteine, and 250 μ M ferrous iron. Immediately after initiating the reaction, spectra were collected every 2 minutes for 120 minutes, and once more the following morning. The results of this time resolved assay, depict a slow progression by which holo-Grx4 evolves after the initial formation of holo-IscU (Figure 2-17). At the conclusion of two hours, the circular dichroism spectra had begun to exhibit features consistent with Grx4, notably the peaks at 315 nm and 555 nm. This coupled with the loss of the 330 nm peak and shoulder region at \sim 500 nm confirms that [2Fe-2S] cluster did indeed transpire, fully visible with the spectra taken 12 hours later, demonstrative of full iron-sulfur cluster turnover solely in the presence of GSH. However, this process required an extensive quantity of time to achieve completion, which is non-physiological and indicates that some fundamental facet of this process is absent. It is highly likely that the mechanism in which GSH provides reducing equivalents is not the primary means in which iron-sulfur clusters are assembled. It may also be possible that the Fdx mediated mechanism of electron donation in the assembly of [2Fe-2S] clusters allows for a more physiologically relevant process.

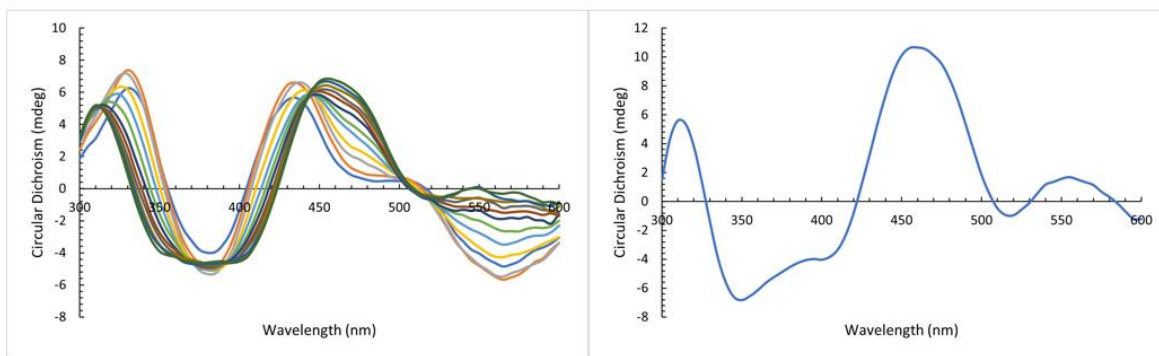


Figure 2-17. Time resolved circular dichroism spectroscopy of [2Fe-2S] cluster assembly and transfer. Assays were conducted with 30 μM IscU, 2 μM IscS, 30 μM Grx4, 100 μM L-cysteine, 250 μM ferrous iron, and 10 mM GSH. Left, spectra collected over the course of 2 hours post reaction initiation, with each trace collected every 10 minutes. Note the emergence of holo-IscU (330 nm) and subsequent loss of spectral features consistent with such (decay of 330 nm into 315 nm). Right, spectrum collected 12 hours post reaction initiation, characteristic of holo-Grx4, with specific peaks at 315 nm and 550 nm, which suggests full cluster transfer from IscU.

Probing the nature of the mechanism of Fdx electron transfer. While the donation of an electron from reduced Fdx to IscS may not bear any physiological significance in the context of iron-sulfur cluster assembly, it is still worthwhile to further characterize elements of its behavior with a known binding partner. The nature of Fdx as a one electron donor is intriguing when coupled with the fact that its target requires two electrons to fully reduce. However, given the indisputable evidence that Fdx can reduce a proteinaceous persulfide, the exact mechanism of this redox event required further analysis. From the lab of John Markley, it was postulated that upon donation of a single electron from Fdx, the persulfide on IscS develops a persulfide anion radical intermediate species.⁴³ However, no experiments were ever conducted to verify this assumption, and currently, no proof for such a mechanism has materialized. To probe the validity of such an intermediate species, radical trapping experiments were carried out using the spin label DMPO. Should a persulfide radical intermediate exist, the DMPO can quench the radical to

create an adduct on IscS detectable with mass spectrometry. To a solution containing IscS, L-cysteine, and reduced Fdx, a 100-fold excess of DMPO was added and allowed to incubate for 30 minutes. Following removal of the spin trap and cleanup of the sample, the material was subjected to ESI mass spectrometry run under denaturing conditions. The results of these excursions, run with varying concentrations of L-cysteine depict a lack of detectable adducts on IscS, consistent across multiple attempts (Figure 2-18). The desired mass shift (48287.01 Da to 48432.23 Da) was never observed, and the only species that was consistently present was IscS with no adduct or even persulfide present on its mobile loop cysteine. These findings suggest that either the formation of this radical species is transient to an extent where it cannot be feasibly trapped with this agent, or that the radical intermediate species does not exist in the first place.

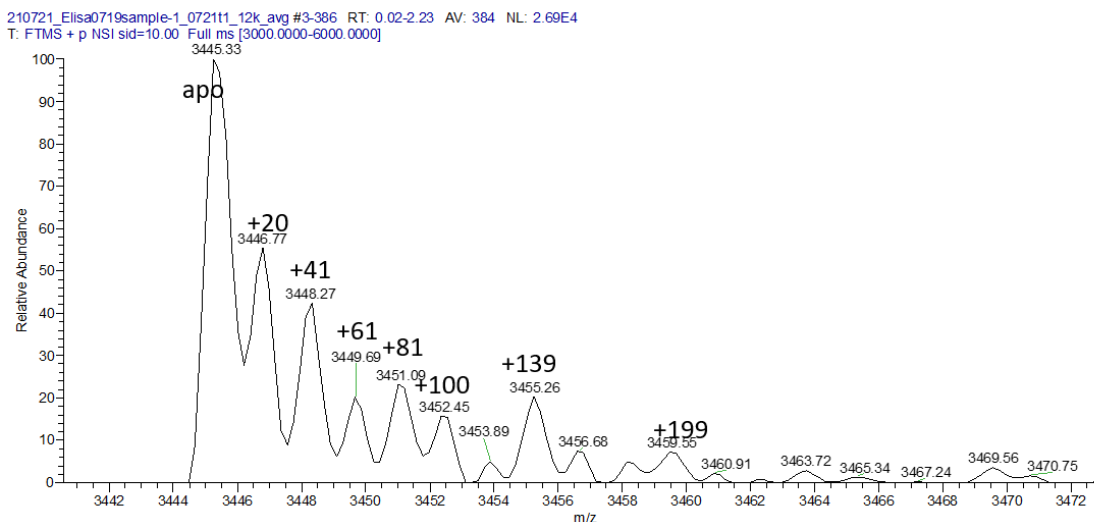


Figure 2-18. Mass spectrum obtained from denaturing conditions of IscS. Experimental conditions featured 10 μ M IscS, 10 μ M reduced Fdx, 50 μ M Cys, and 1 mM DMPO. The major peak observed is apo-IscS, or IscS with no persulfide or adduct on its catalytic cysteine. This peak, with a m/z of 3445.33, is the only peak of significant intensity. No mass shifts corresponding to the mass shift of a DMPO adduct were detected.

2.4. Discussion

Based on the results presented, it can be concluded that the oxidation event of Fdx observed in the *in vitro* assays conducted represents a potentially off path, non-viable mechanism in the biological assembly of [2Fe-2S] clusters. Rather, what has been studied is just one facet of the behavior of a protein which still requires additional research to properly elucidate its fully physiological functionality. The most fitting explanation for the behavior witnessed is that the setting of solely IscS, Fdx, and L-cysteine in solution is not an environment conducive to analyzing the behavior of Fdx, as the absence of other proteins in the iron-sulfur protein assembly complex may be contributing to a perceived inability for the protein to oxidize readily. The lag phase described in the results may be a consequence of several factors, with the most likely possibility that excess cysteine in solution is behaving as a competing reductant and cleaving the persulfide formed on IscS before reduced Fdx can bind and perform that process itself. This scenario would explain why the lag times consistently lengthened in duration as the concentrations of cysteine administered increased. The lag phase is most likely representative of the amount of time needed for Fdx to finally interact with a persulfide on IscS C328 that has not been perturbed by any free floating cysteine. With less cysteine in solution to compete with Fdx for the persulfide on the C328 residue, the lag phase is found to be shorter. The preincubation times added into assays accomplishes a similar feat—exhaust free cysteine that would cleave the persulfide on IscS, leaving behind free targets for Fdx redox activity upon its eventual addition. Taken together, the major takeaway from these experiments in addition to the lag phase was the fact that Fdx shows an ability to reduce the persulfide on IscS, in accordance with what was presented in Kim et al. 2013. These results have gone further to definitively establish such,

utilizing multiple IcsS mutants (C328 and C110A, C170A) along with a thiol reductant in TCEP to firmly establish the persulfide on C328 as the target for Fdx electron donation. How precisely Fdx is able to reductively cleave this persulfide from a mechanistic standpoint remains elusive, as attempts to scour for a radical intermediate have not borne fruit. Endeavors with denaturing mass spectrometry were unable to detect an adduct on IcsS, either due to the transient nature of this radical species, or its fundamental non-existence.

In regards to the role of reduced Fdx in the context of iron-sulfur cluster assembly, the aforementioned experimentation was able to conclusively establish that Fdx can take up the role as the reductant in this process; assays conducted with circular dichroism spectroscopy ascertained that [2Fe-2S] clusters can be generated on IcsU as the redox state of Fdx changes, an observation not examined previously in the established literature. However, on account of the fact that the Fdx oxidation does not perfectly correlate with the formation of iron-sulfur clusters, there remain additional questions onto what precisely is transpiring when the oxidation state of Fdx is changing under these circumstances. In spite of this, it was observed that holo-IcsU incidence is not preceded by any kind of lag phase, indicative that the behavior of Fdx with just IcsS and cysteine alone is not physiologically relevant, as it fails to establish catalytic competence with its extended lag phase. Investigation that incorporated the small molecule thiol glutathione only exacerbated the mystery behind the role of the reductant in iron-sulfur cluster assembly, as GSH alone was proven to be sufficient for the full turnover of a [2Fe-2S] cluster onto the carrier protein Grx4, albeit quite slowly. Yet, *in vivo* studies conducted in *E.coli* previously have uncovered a strict necessity for Fdx in the biosynthesis of iron-sulfur clusters. The interplay between Fdx and GSH presents a new wrinkle in the swirl of questions surrounding the identity of the physiological reductant for this biological process, with no

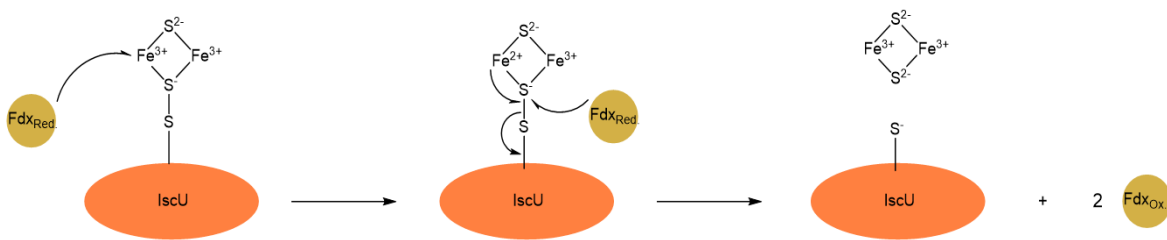


Figure 2-19. Proposed model of Fdx mediated reduction for iron-sulfur cluster assembly on IscU. In this proposed mechanism, Fdx is postulated to act later in the [2Fe-2S] assembly process, when an immature cluster is still tethered to the scaffold protein IscU by a persulfide. Reduced Fdx can reduce one of the ferric irons to its ferrous form. An electron from this iron, along with one from a second reduced Fdx can proceed to cleave the persulfide, resulting in the release of a mature [2Fe-2S] cluster.

decisive answers able to put forth at this point. However, from what can be gleaned from the aforementioned results, possible models of how Fdx and GSH behave in the context of this process are proposed. It is possible that Fdx is acting at a later stage of [2Fe-2S] cluster assembly, either cleaving the final persulfide linkage that tethers the nascent cluster to IscU, or providing a source of reducing equivalents to convert the ferric irons to their ferrous forms, which in turn facilitates the flow of electrons to properly reduce the sulfurs to their sulfide state (Figure 2-19). In Gervason et al. 2019, the persulfidation experiment was able to identify the persulfide on ISCU2 as the potential target of electron donation from FDX2, which may be the case for the *E. coli* Fdx as well. As for the role of GSH, it is harder to identify where it may act; as a two electron donor, it can easily cleave the persulfide on IscS or afterwards when it is transferred to IscU (Figure 2-20). Native mass spectrometry experiments conducted in this laboratory that also incorporated GSH were unsuccessful in assigning this thiol an exact role, as the expected GSH adducts that would form were it to cleave the persulfide on IscU were not detected at appreciable levels consistent with that mechanism. Further experimentation needs to

be performed in order to properly gauge the role of GSH, and to ascertain whether it is a secondary reductant, or a thiol that serves a role solely in the downstream component of iron-sulfur cluster assembly.

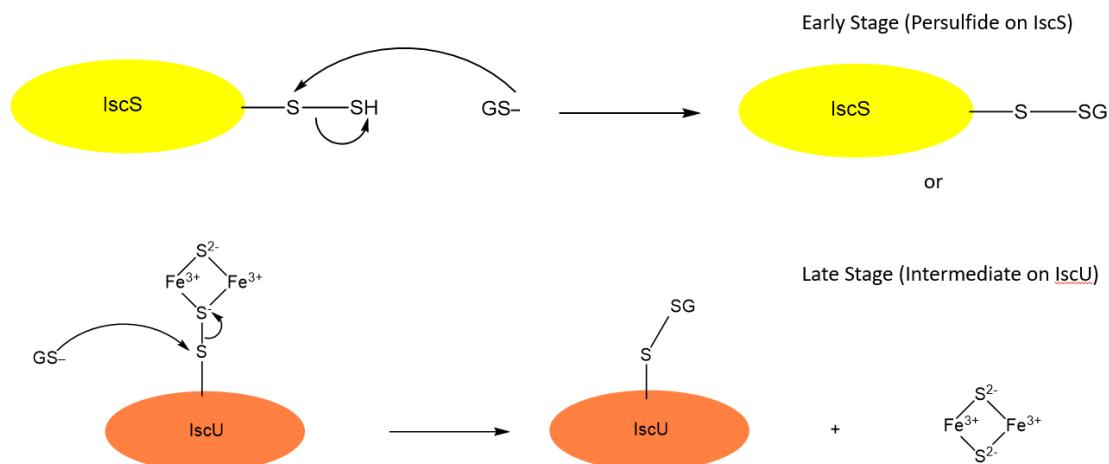


Figure 2-20. Proposed model of GSH mediated iron-sulfur cluster assembly. With the ability to perform two electron chemistry, GSH may behave early on in iron-sulfur cluster assembly by cleaving the initial persulfide that forms on IscS. However, it may also have the capacity to act later on, to liberate immature [2Fe-2S] clusters from the scaffold protein IscU by cleaving the persulfide that links them to the protein.

An unfortunate setback that prevented greater insight into a more physiologically relevant iron-sulfur cluster assembly assay was the inability to utilize the natural source of electrons for Fdx, its corresponding ferredoxin NADP reductase. For reasons not quite understood, in this laboratory, reduction of Fdx was unable to be attained solely using NADPH and the reductase, despite the fact that the two proteins exhibited otherwise normal behavior in nearly all other capacities. This left the assays conducted reliant on utilizing artificial means to reduce Fdx, and subsequently prevented a physiologically meaningful regeneration system for Fdx, where

oxidized protein would be re-reduced by the reductase. On account of this, it remains to be seen whether the inclusion of this reductase would potentially resolve the conundrum in which the redox activity of Fdx did not quite correlate with the observed formation of holo-IscU.

3. CONCLUSIONS

The work conducted in this laboratory was performed with the goal of expanding the currently understood behavior of the *E. coli* [2Fe-2S] ferredoxin, Fdx, a protein that has yet to be assigned a definitive functional role. In the context of physiologically relevant iron-sulfur cluster assembly, there still remain pertinent questions to be addressed, but what has transpired in this laboratory has hopefully served to shed light on phenomena attributed to Fdx in an *in vitro* setting. What this research has uncovered is that the mechanism previously proposed for Fdx in the context of *E. coli* iron-sulfur cluster biosynthesis is mostly likely an *in vitro* phenomenon that is not reflective of the physiological occurrence. It has been established that under these circumstances, Fdx is donating its electrons to the persulfide of IscS in a manner akin to a potentially off path reaction that may not contribute meaningfully to providing the two electrons necessary for the assembly of a [2Fe-2S] cluster.

In spite of this, the redox activity of Fdx presented in this work is still a facet of the protein's functionality and has warranted the additional study that was presented in the previous chapter. Despite attempts to characterize the specifics of this mechanism of electron transfer from Fdx to IscS, exact details remain uncertain, as confirmation of a proposed radical intermediate species was unable to be achieved. While the precise role of this protein remains elusive, attention can be focused towards alternative endeavors in order to uncover the true mechanism by which the necessary reducing equivalents are donated for the assembly of a [2Fe-2S] cluster. Incorporation of the ferredoxin NADP reductase into iron-sulfur cluster assembly would prove useful to discern the effect of a physiological regeneration system has on the behavior of Fdx and whether the results presented in Chapter 2 remain valid. Further exploration of the role and potential contribution from GSH is warranted, as the possibility of a secondary reductant for iron-sulfur

cluster assembly cannot be discounted. It may be that on account of the paradoxical nature of employing a [2Fe-2S] protein to assemble [2Fe-2S] clusters that GSH exists to facilitate a form of iron-sulfur cluster assembly that is Fdx independent, though the *in vivo* data previously discussed would suggest that such a process would be by no means the primary means for biosynthesis of iron-sulfur clusters. Additional spectroscopic endeavors can perhaps solve this conundrum and bring the field closer to resolving the mystery surrounding *E.coli* Fdx and its homologues.

REFERENCES

1. Fontecave, M. Iron-sulfur clusters: ever-expanding roles. *Nat Chem Biol* **2**, 171–174 (2006).
2. Beinert, H. Iron-Sulfur Proteins: Ancient Structures, Still Full of Surprises. *J. Biol. Inorg. Chem.* **2000**, 5 (1), 2–15.
3. Cardenas-Rodriguez, M.; Chatzi, A.; Tokatlidis, K. Iron-Sulfur Clusters: From Metals through Mitochondria Biogenesis to Disease. *J. Biol. Inorg. Chem.* **2018**, 23 (4), 509–520.
4. Tsaousis, A. D. On the Origin of Iron/Sulfur Cluster Biosynthesis in Eukaryotes. *Front. Microbiol.* **2019**, 10, 2478.
5. Johnson, D. C.; Dean, D. R.; Smith, A. D.; Johnson, M. K. Structure, Function, and Formation of Biological Iron-Sulfur Clusters. *Annu. Rev. Biochem.* **2005**, 74 (1), 247–281.
6. Zheng, L.; Cash, V. L.; Flint, D. H.; Dean, D. R. Assembly of Iron-Sulfur Clusters. *J. Biol. Chem.* **1998**, 273 (21), 13264–13272.
7. Takahashi, Y.; Nakamura, M. Functional Assignment of the ORF2-IscS-IscU-IscA-HscB-HscA-Fdx-ORF3 Gene Cluster Involved in the Assembly of Fe-S Clusters in Escherichia Coli. *J. Biochem.* **1999**, 126 (5), 917–926.

8. Tokumoto, U.; Takahashi, Y. Genetic Analysis of the Isc Operon in Escherichia Coli Involved in the Biogenesis of Cellular Iron-Sulfur Proteins. *J. Biochem.* **2001**, *130* (1), 63–71.
9. Tokumoto, U.; Nomura, S.; Minami, Y.; Mihara, H.; Kato, S.-I.; Kurihara, T.; Esaki, N.; Kanazawa, H.; Matsubara, H.; Takahashi, Y. Network of Protein-Protein Interactions among Iron-Sulfur Cluster Assembly Proteins in Escherichia Coli. *J. Biochem.* **2002**, *131* (5), 713–719.
10. Averill, B. A.; Herskovitz, T.; Holm, R. H.; Ibers, J. A. ChemInform Abstract: SYNTHETIC ANALOGS OF THE ACTIVE SITES OF IRON-SULFUR PROTEINS PART 2, SYNTHESIS AND STRUCTURE OF THE TETRA(MERCAPTO-MU(3)-SULFIDO-IRON) CLUSTERS, (FE₄S₄(SR)₄)(²⁻). *Chem. Inf.* **1973**, *4* (32), no-no.
11. Herskovitz, T.; Averill, B. A.; Holm, R. H.; Ibers, J. A.; Phillips, W. D.; Weiher, J. F. Structure and Properties of a Synthetic Analogue of Bacterial Iron-Sulfur Proteins. *Proceedings of the National Academy of Sciences* **1972** *69* (9), 2437–2441.
12. Lill, R.; Mühlenhoff, U. Maturation of Iron-Sulfur Proteins in Eukaryotes: Mechanisms, Connected Processes, and Diseases. *Annu. Rev. Biochem.* **2008**, *77* (1), 669–700.

13. Lill, R.; Broderick, J. B.; Dean, D. R. Special Issue on Iron-Sulfur Proteins: Structure, Function, Biogenesis and Diseases. *Biochim. Biophys. Acta* **2015**, *1853* (6), 1251–1252.
14. Choudens, S.; Barras, F. G. Biochemical, and Biophysical Methods for Studying Fe S Proteins and Their Assembly; 2017.
15. Ollagnier-de-Choudens, S.; Mattioli, T.; Takahashi, Y.; Fontecave, M. Iron-Sulfur Cluster Assembly: CHARACTERIZATION OF IscA AND EVIDENCE FOR A SPECIFIC AND FUNCTIONAL COMPLEX WITH FERREDOXIN. *J. Biol. Chem.* **2001**, *276* (25), 22604–22607.
16. Py, B.; Barras, F. Building Fe–S Proteins: Bacterial Strategies. *Nat. Rev. Microbiol.* **2010**, *8* (6), 436–446.
17. Blanc, B.; Gerez, C.; Ollagnier de Choudens, S. Assembly of Fe/S Proteins in Bacterial Systems. *Biochim. Biophys. Acta Mol. Cell Res.* **2015**, *1853* (6), 1436–1447.
18. Roche, B.; Aussel, L.; Ezraty, B.; Mandin, P.; Py, B.; Barras, F. Iron/Sulfur Proteins Biogenesis in Prokaryotes: Formation, Regulation and Diversity. *Biochim. Biophys. Acta Bioenerg.* **2013**, *1827* (3), 455–469.
19. Kessler, P. S.; Blank, C.; Leigh, J. A. The Nif Gene Operon of the Methanogenic Archaeon *Methanococcus Maripaludis*. *J. Bacteriol.* **1998**, *180* (6), 1504–1511.

20. Xu, X. M.; Møller, S. G. Iron–Sulfur Clusters: Biogenesis, Molecular Mechanisms, and Their Functional Significance. *Antioxid. Redox Signal.* **2011**, *15* (1), 271–307.
21. Baussier, C.; Fakroun, S.; Aubert, C.; Dubrac, S.; Mandin, P.; Py, B.; Barras, F. Making Iron-Sulfur Cluster: Structure, Regulation and Evolution of the Bacterial ISC System. In *Advances in Agronomy*; Elsevier, 2020; pp 1–39.
22. Ayala-Castro, C.; Saini, A.; Outten, F. W. Fe-S Cluster Assembly Pathways in Bacteria. *Microbiol. Mol. Biol. Rev.* **2008**, *72* (1), 110–125, table of contents.
23. Bai, Y.; Chen, T.; Happe, T.; Lu, Y.; Sawyer, A. Iron–Sulphur Cluster Biogenesis via the SUF Pathway. *Metallomics* **2018**, *10* (8), 1038–1052.
24. Kim, J. H.; Bothe, J. R.; Alderson, T. R.; Markley, J. L. Tangled Web of Interactions among Proteins Involved in Iron–Sulfur Cluster Assembly as Unraveled by NMR, SAXS, Chemical Crosslinking, and Functional Studies. *Biochim. Biophys. Acta Mol. Cell Res.* **2015**, *1853* (6), 1416–1428.
25. Nakamura, M.; Saeki, K.; Takahashi, Y. Hyperproduction of Recombinant Ferredoxins in Escherichia Coli by Coexpression of the OKFI-ORF2-IscS-IscU-IscA-HscB-HscA-Fdx-ORF3 Gene Cluster. *J. Biochem* **1999**, *126* (1), 9.
26. Schwartz, C. J.; Giel, J. L.; Patschkowski, T.; Luther, C.; Ruzicka, F. J.; Beinert, H.; Kiley, P. J. IscR, an Fe-S Cluster-Containing Transcription Factor, Represses Expression of Escherichia Coli Genes Encoding Fe-S Cluster Assembly Proteins. *Proc. Natl. Acad. Sci. U. S. A.* **2001**, *98* (26), 14895–14900.

27. Yeo, W.-S.; Lee, J.-H.; Lee, K.-C.; Roe, J.-H. IscR Acts as an Activator in Response to Oxidative Stress for the Suf Operon Encoding Fe-S Assembly Proteins: Positive Regulation of The suf Operon by IscR. *Mol. Microbiol.* **2006**, *61* (1), 206–218.
28. Giel, J. L.; Rodionov, D.; Liu, M.; Blattner, F. R.; Kiley, P. J. IscR-Dependent Gene Expression Links Iron-Sulphur Cluster Assembly to the Control of O₂-Regulated Genes in Escherichia Coli. *Mol. Microbiol.* **2006**, *60* (4), 1058–1075.
29. Fleischhacker, A. S.; Stubna, A.; Hsueh, K.-L.; Guo, Y.; Teter, S. J.; Rose, J. C.; Brunold, T. C.; Markley, J. L.; Münck, E.; Kiley, P. J. Characterization of the [2Fe-2S] Cluster of Escherichia Coli Transcription Factor IscR. *Biochemistry* **2012**, *51* (22), 4453–4462.
30. Urbina, H. D.; Silberg, J. J.; Hoff, K. G.; Vickery, L. E. Transfer of Sulfur from IscS to IscU during Fe/S Cluster Assembly. *J. Biol. Chem.* **2001**, *276* (48), 44521–44526.
31. Bonomi, F.; Iametti, S.; Ta, D.; Vickery, L. E. Multiple Turnover Transfer of [2Fe2S] Clusters by the Iron-Sulfur Cluster Assembly Scaffold Proteins IscU and IscA. *J. Biol. Chem.* **2005**, *280* (33), 29513–29518.
32. Zeng, J.; Geng, M.; Jiang, H.; Liu, Y.; Liu, J.; Qiu, G. The IscA from Acidithiobacillus Ferrooxidans Is an Iron-Sulfur Protein Which Assemble the [Fe₄S₄] Cluster with Intracellular Iron and Sulfur. *Arch. Biochem. Biophys.* **2007**, *463* (2), 237–244.

33. Vinella, D.; Brochier-Armanet, C.; Loiseau, L.; Talla, E.; Barras, F. Iron-Sulfur (Fe/S) Protein Biogenesis: Phylogenomic and Genetic Studies of A-Type Carriers. *PLoS Genet.* **2009**, *5* (5), e1000497.
34. Dutkiewicz, R.; Nowak, M.; Craig, E. A.; Marszalek, J. Fe-S Cluster Hsp70 Chaperones: The ATPase Cycle and Protein Interactions. *Methods Enzymol.* **2017**, *595*, 161–184.
35. Mayer, M. P.; Gierasch, L. M. Recent Advances in the Structural and Mechanistic Aspects of Hsp70 Molecular Chaperones. *J. Biol. Chem.* **2019**, *294* (6), 2085–2097.
36. Bonomi, F.; Iametti, S.; Morleo, A.; Ta, D.; Vickery, L. E. Studies on the Mechanism of Catalysis of Iron–Sulfur Cluster Transfer from IscU[2Fe2S] by HscA/HscB Chaperones. *Biochemistry* **2008**, *47* (48), 12795–12801.
37. Puglisi, R.; Pastore, A. The Role of Chaperones in Iron–Sulfur Cluster Biogenesis. *FEBS Lett.* **2018**, *592* (24), 4011–4019.
38. Lange, H.; Kaut, A.; Kispal, G.; Lill, R. A Mitochondrial Ferredoxin Is Essential for Biogenesis of Cellular Iron-Sulfur Proteins. *Proc. Natl. Acad. Sci. U. S. A.* **2000**, *97* (3), 1050–1055.
39. Kim, J. H.; Frederick, R. O.; Reinen, N. M.; Troupis, A. T.; Markley, J. L. [2Fe-2S]-Ferredoxin Binds Directly to Cysteine Desulfurase and Supplies an Electron for Iron–Sulfur Cluster Assembly but Is Displaced by the Scaffold Protein or Bacterial Frataxin. *J. Am. Chem. Soc.* **2013**, *135* (22), 8117–8120.

<https://pubs.acs.org/doi/10.1021/ja401950a>. Further permission related to the material excerpted should be directed to the ACS.

40. Weibert, H.; Freibert, S.-A.; Gallo, A.; Heidenreich, T.; Linne, U.; Amlacher, S.; Hurt, E.; Mühlenhoff, U.; Banci, L.; Lill, R. Functional Reconstitution of Mitochondrial Fe/S Cluster Synthesis on Isu1 Reveals the Involvement of Ferredoxin. *Nat. Commun.* **2014**, *5* (1). <https://doi.org/10.1038/ncomms6013>.
41. Cai, K.; Tonelli, M.; Frederick, R. O.; Markley, J. L. Human Mitochondrial Ferredoxin 1 (FDX1) and Ferredoxin 2 (FDX2) Both Bind Cysteine Desulfurase and Donate Electrons for Iron-Sulfur Cluster Biosynthesis. *Biochemistry* **2017**, *56* (3), 487–499. Further permission related to the material excerpted should be directed to the ACS.
42. Shimomura, Y.; Takahashi, Y.; Kakuta, Y.; Fukuyama, K. Crystal Structure of Escherichia Coli YfhJ Protein, a Member of the ISC Machinery Involved in Assembly of Iron-Sulfur Clusters. *Proteins* **2005**, *60* (3), 566–569.
43. Kim, J. H.; Bothe, J. R.; Frederick, R. O.; Holder, J. C.; Markley, J. L. Role of IscX in Iron–Sulfur Cluster Biogenesis in Escherichia Coli. *J. Am. Chem. Soc.* **2014**, *136* (22), 7933–7942.
44. Pastore, C.; Adinolfi, S.; Huynen, M. A.; Rybin, V.; Martin, S.; Mayer, M.; Bukau, B.; Pastore, A. YfhJ, a Molecular Adaptor in Iron-Sulfur Cluster Formation or a Frataxin-like Protein? *Structure* **2006**, *14* (5), 857–867.

45. Adinolfi, S.; Puglisi, R.; Crack, J. C.; Iannuzzi, C.; Dal Piaz, F.; Konarev, P. V.; Svergun, D. I.; Martin, S.; Le Brun, N. E.; Pastore, A. Molecular Mechanism of the Dual Regulation of Bacterial Iron Sulfur Cluster Biogenesis by CyaY and IscX, 2017. <https://doi.org/10.1101/212290>.
46. Tanaka, N.; Yuda, E.; Fujishiro, T.; Hirabayashi, K.; Wada, K.; Takahashi, Y. Identification of IscU Residues Critical for de Novo Iron–Sulfur Cluster Assembly. *Mol. Microbiol.* **2019**, *112* (6), 1769–1783.
47. Kim, J. H.; Tonelli, M.; Kim, T.; Markley, J. L. Three-Dimensional Structure and Determinants of Stability of the Iron–Sulfur Cluster Scaffold Protein IscU from Escherichia Coli. *Biochemistry* **2012**, *51* (28), 5557–5563.
48. Kim, J. H.; Füzéry, A. K.; Tonelli, M.; Ta, D. T.; Westler, W. M.; Vickery, L. E.; Markley, J. L. Structure and Dynamics of the Iron–Sulfur Cluster Assembly Scaffold Protein IscU and Its Interaction with the Cochaperone HscB. *Biochemistry* **2009**, *48* (26), 6062–6071.
49. Kakuta, Y.; Horio, T.; Takahashi, Y.; Fukuyama, K. Crystal Structure of Escherichia Coli Fdx, an Adrenodoxin-Type Ferredoxin Involved in the Assembly of Iron–Sulfur Clusters. *Biochemistry* **2001**, *40* (37), 11007–11012.
50. Knoell, H. E.; Knappe, J. Escherichia Coli Ferredoxin, an Iron-Sulfur Protein of the Adrenodoxin Type. *Eur. J. Biochem.* **1974**, *50* (1), 245–252.

51. Ta, D. T.; Vickery, L. E. Cloning, Sequencing, and Overexpression of a [2Fe-2S] Ferredoxin Gene from Escherichia Coli. *J. Biol. Chem.* **1992**, *267* (16), 11120–11125.
52. Yan, R.; Adinolfi, S.; Iannuzzi, C.; Kelly, G.; Oregioni, A.; Martin, S.; Pastore, A. Cluster and Fold Stability of E. Coli ISC-Type Ferredoxin. *PLoS One* **2013**, *8* (11), e78948.
53. Holden, H. M.; Jacobson, B. L.; Hurley, J. K.; Tollin, G.; Oh, B.-H.; Skjeldal, L.; Chae, Y. K.; Cheng, H.; Xia, B.; Markley, J. L. Structure-Function Studies of [2Fe-2S] Ferredoxins. *J. Bioenerg. Biomembr.* **1994**, *26* (1), 67–88.
54. Wan, J. T.; Jarrett, J. T. Electron Acceptor Specificity of Ferredoxin (FLavodoxin):NADPp Oxidoreductase from Escherichia Coliq. *Archives of Biochemistry and Biophysics* **2002**.
55. Yan, R.; Adinolfi, S.; Pastore, A. Ferredoxin, in Conjunction with NADPH and Ferredoxin-NADP Reductase, Transfers Electrons to the IscS/IscU Complex to Promote Iron–Sulfur Cluster Assembly. *Biochim. Biophys. Acta Proteins Proteom.* **2015**, *1854* (9), 1113–1117.
56. Chandramouli, K.; Unciuleac, M.-C.; Naik, S.; Dean, D. R.; Huynh, B. H.; Johnson, M. K. Formation and Properties of [4Fe-4S] Clusters on the IscU Scaffold Protein. *Biochemistry* **2007**, *46* (23), 6804–6811.
57. Yan, R.; Konarev, P. V.; Iannuzzi, C.; Adinolfi, S.; Roche, B.; Kelly, G.; Simon, L.; Martin, S. R.; Py, B.; Barras, F.; Svergun, D. I.; Pastore, A. Ferredoxin

- Competes with Bacterial Frataxin in Binding to the Desulfurase IscS. *J. Biol. Chem.* **2013**, 288 (34), 24777–24787.
58. Barros, M. H.; Nobrega, F. G. YAH1 of *Saccharomyces Cerevisiae*: A New Essential Gene That Codes for a Protein Homologous to Human Adrenodoxin. *Gene* **1999**, 233 (1–2), 197–203.
59. Mühlenhoff, U.; Gerber, J.; Richhardt, N.; Lill, R. Components Involved in Assembly and Dislocation of Iron-Sulfur Clusters on the Scaffold Protein Isu1p. *EMBO J.* **2003**, 22 (18), 4815–4825.
60. Alves, R.; Herrero, E.; Sorribas, A. Predictive Reconstruction of the Mitochondrial Iron-Sulfur Cluster Assembly Metabolism: I. The Role of the Protein Pair Ferredoxin-Ferredoxin Reductase (Yah1-Arh1). *Proteins* **2004**, 56 (2), 354–366.
61. Sheftel, A. D.; Stehling, O.; Pierik, A. J.; Elsässer, H.-P.; Mühlenhoff, U.; Webert, H.; Hobler, A.; Hannemann, F.; Bernhardt, R.; Lill, R. Humans Possess Two Mitochondrial Ferredoxins, Fdx1 and Fdx2, with Distinct Roles in Steroidogenesis, Heme, and Fe/S Cluster Biosynthesis. *Proc. Natl. Acad. Sci. U. S. A.* **2010**, 107 (26), 11775–11780.
62. Shi, Y.; Ghosh, M.; Kovtunovych, G.; Crooks, D. R.; Rouault, T. A. Both Human Ferredoxins 1 and 2 and Ferredoxin Reductase Are Important for Iron-Sulfur Cluster Biogenesis. *Biochim. Biophys. Acta* **2012**, 1823 (2), 484–492.

63. Lill, R.; Freibert, S.-A. Mechanisms of Mitochondrial Iron-Sulfur Protein Biogenesis. *Annu. Rev. Biochem.* **2020**, *89* (1), 471–499.
64. Jung, Y. S.; Gao-Sheridan, H. S.; Christiansen, J.; Dean, D. R.; Burgess, B. K. Purification and Biophysical Characterization of a New [2Fe-2S] Ferredoxin from *Azotobacter Vinelandii*, a Putative [Fe-S] Cluster Assembly/Repair Protein. *J. Biol. Chem.* **1999**, *274* (45), 32402–32410.
65. Gurgel-Giannetti, J.; Lynch, D. S.; Paiva, A. R. B. de; Lucato, L. T.; Yamamoto, G.; Thomsen, C.; Basu, S.; Freua, F.; Giannetti, A. V.; de Assis, B. D. R.; Ribeiro, M. D. O.; Barcelos, I.; Sayão Souza, K.; Monti, F.; Melo, U. S.; Amorim, S.; Silva, L. G. L.; Macedo-Souza, L. I.; Vianna-Morgante, A. M.; Hirano, M.; Van der Knaap, M. S.; Lill, R.; Vainzof, M.; Oldfors, A.; Houlden, H.; Kok, F. A Novel Complex Neurological Phenotype Due to a Homozygous Mutation in FDX2. *Brain* **2018**, *141* (8), 2289–2298.
66. Spiegel, R.; Saada, A.; Halvardson, J.; Soiferman, D.; Shaag, A.; Edvardson, S.; Horovitz, Y.; Khayat, M.; Shalev, S. A.; Feuk, L.; Elpeleg, O. Deleterious Mutation in FDX1L Gene Is Associated with a Novel Mitochondrial Muscle Myopathy. *Eur. J. Hum. Genet.* **2014**, *22* (7), 902–906.
67. Gervason, S.; Larkem, D.; Mansour, A. B.; Botzanowski, T.; Müller, C. S.; Pecqueur, L.; Le Pavec, G.; Delaunay-Moisan, A.; Brun, O.; Agramunt, J.; Grandas, A.; Fontcave, M.; Schünemann, V.; Cianférani, S.; Sizun, C.; Tolédano, M. B.; D’Autréaux, B. Physiologically Relevant Reconstitution of

- Iron-Sulfur Cluster Biosynthesis Uncovers Persulfide-Processing Functions of Ferredoxin-2 and Frataxin. *Nat. Commun.* **2019**, *10* (1), 3566.
68. Lin, C.-W.; McCabe, J. W.; Russell, D. H.; Barondeau, D. P. Molecular Mechanism of ISC Iron-Sulfur Cluster Biogenesis Revealed by High-Resolution Native Mass Spectrometry. *J. Am. Chem. Soc.* **2020**, *142* (13), 6018–6029.
69. Vranish, J. N.; Russell, W. K.; Yu, L. E.; Cox, R. M.; Russell, D. H.; Barondeau, D. P. Fluorescent Probes for Tracking the Transfer of Iron-Sulfur Cluster and Other Metal Cofactors in Biosynthetic Reaction Pathways. *J. Am. Chem. Soc.* **2015**, *137* (1), 390–398.
70. Vranish, J. N.; Das, D.; Barondeau, D. P. Real-Time Kinetic Probes Support Monothiol Glutaredoxins as Intermediate Carriers in Fe–S Cluster Biosynthetic Pathways. *ACS Chem. Biol.* **2016**, *11* (11), 3114–3121.
71. Fox, N. G.; Das, D.; Chakrabarti, M.; Lindahl, P. A.; Barondeau, D. P. Frataxin Accelerates [2Fe-2S] Cluster Formation on the Human Fe-S Assembly Complex. *Biochemistry* **2015**, *54* (25), 3880–3889.
72. Seefeldt, L. C.; Ensign, S. A. A Continuous, Spectrophotometric Activity Assay for Nitrogenase Using the Reductant Titanium(III) Citrate. *Anal. Biochem.* **1994**, *221* (2), 379–386.
73. Lauhon, C. T.; Kambampati, R. The *IscS* Gene in *Escherichia Coli* Is Required for the Biosynthesis of 4-Thiouridine, Thiamin, and NAD. *J. Biol. Chem.* **2000**, *275* (26), 20096–20103

74. Patra, S.; Barondeau, D. P. Mechanism of Activation of the Human Cysteine Desulfurase Complex by Frataxin. *Proc. Natl. Acad. Sci. U. S. A.* 2019, 116 (39), 19421–19430.
75. Fahey, R. C.; Brown, W. C.; Adams, W. B.; Worsham, M. B. Occurrence of Glutathione in Bacteria. *J. Bacteriol.* 1978, 133 (3), 1126–1129.
76. Daniel, T.; Faruq, H. M.; Laura Magdalena, J.; Manuela, G.; Christopher Horst, L. Role of GSH and Iron-Sulfur Glutaredoxins in Iron Metabolism-Review. *Molecules* 2020, 25 (17), 3860.
77. McLaggan, D.; Logan, T. M.; Lynn, D. G.; Epstein, W. Involvement of Gamma-Glutamyl Peptides in Osmoadaptation of Escherichia Coli. *J. Bacteriol.* 1990, 172 (7), 3631–3636.
78. Burns, J. A.; Butler, J. C.; Moran, J.; Whitesides, G. M. Selective Reduction of Disulfides by Tris(2-Carboxyethyl)Phosphine. *J. Org. Chem.* 1991, 56 (8), 2648–2650